8-1991

ETA Photoproduction VIA $^{2}H(\gamma\eta)^{2}H^{*}$

Yan Zhang
Western Michigan University

ETA PHOTOPRODUCTION VIA $^2H(\gamma,\eta)^2H^*$

by

Yan Zhang

A Thesis
Submitted to the
Faculty of The Graduate College
in partial fulfillment of the
requirements for the
Degree of Master of Arts
Department of Physics

Western Michigan University
Kalamazoo, Michigan
August 1991

ETA PHOTOPRODUCTION VIA $^2H(\gamma,\eta)^2H^*$

Yan Zhang, M.A.

Western Michigan University, 1991

The reaction $^2H(\gamma,\eta)^2H^*$ is studied using the impulse approximation. A recent fit to the $^1H(\gamma,\eta)^1H$ elementary amplitude is employed in the calculation. The n-p final state is described by Reid's soft core potentials. The calculation shows very different cross sections for the final isospin 0 and isospin 1 break-up channels. The S_{11} resonance is demonstrated to dominate the eta cross sections in the 740 MeV photon laboratory energy region. Fermi motion in the deuteron does not significantly spread the effect of the S_{11}. All these results demonstrate that the reaction $^2H(\gamma,\eta)^2H^*$ may provide a signature for the isospin components of the S_{11} electromagnetic transition amplitude. Measurement of this reaction will complement the earlier $^2H(\gamma,\eta)^2H$ data.

ACKNOWLEDGMENTS

I wish to express my infinite gratitude and sincere appreciation to my advisor, Professor Dean Halderson, for suggesting the topic of this thesis, and for all of his direction, encouragement and great help throughout the course of this research. It is with pleasure that I also thank the other members of my committee, Professor Alvin Rosenthal and Professor Michitoshi Soga, for their valuable advice and help.

Yan Zhang

Order Number 1345534

Eta photoproduction via $^2H(\gamma,\eta)^2H^*$

Zhang, Yan, M.A.

Western Michigan University, 1991

U·M·I
300 N. Zeeb Rd.
Ann Arbor, MI 48106

TABLE OF CONTENTS

LIST OF TABLES

LIST OF FIGURES

List of Figures-Continued

CHAPTER I

INTRODUCTION

Photoproduction and electroproduction of mesons from nucleon are an important part of studies of nucleon resonances because meson emission is the dominant channel. By comparing the experimental electromagnetic transition amplitudes with the quark model predictions, the validity of quark models in describing nucleon resonances can be tested, and therefore a better understanding of the underlying structure of these resonances can be achieved. With new experimental facilities (e.g., CEBAF), interest in meson photoproduction has been renewed. Although the majority of experiments investigated charged pion productions, more data on the photoproduction of eta mesons are expected due to the recently developed neutral meson detectors.[1] The S_{11} (1535) resonance, with its large eta decay width (45%), can then be isolated for study by these eta-production experiments.

The T-matrix for eta photoproduction from the nucleon can be written in isospin components as:

$$T = T^0 + \tau_3 T^1 , \qquad (1.1)$$

where $\tau_3|p\rangle = -|p\rangle$.

Because the strong ηN interaction in the final states does not distinguish between the neutron and proton, the T^0 and T^1 represent just isospin components of electromagnetic transition amplitudes for nucleon resonances. Obviously, these isospin components must be obtained from experiments with both proton and neutron targets. Neutron data can only come from nuclear targets. Although the data extracted from early photopion experiments[2] indicated that electromagnetic amplitude of the S_{11} resonance is nearly pure isovector, in agreement with quark model predictions,[3,4] early data from photoproduction of eta on a deuteron target[5] were analyzed in the impulse approximation to give a nearly pure isoscalar transition amplitude. Some efforts have been made to explain this discrepancy by meson rescattering effects.[6] However, the most recent calculation of the rescattering diagrams[7] indicated that they are too small to account for the difference. In that article, the angular distributions of $^2H(\gamma,\eta)^2H$ were suggested as a means of distinguishing between the single scattering and meson rescattering processes. The difficulty is the low yield of $^2H(\gamma,\eta)^2H$ due to the inability of the deuteron to accommodate the high momentum transfer in the reaction. It was also suggested by Halderson and Rosenthal[8] to determine the isospin components of the S_{11} resonance by photoproduction

of eta mesons from excited, stretched states of several nuclei. The nucleus would be used as an isospin filter. However, the considerable Fermi motion of nucleons in these heavy nuclei tends to smear out the contributions of individual nucleon resonances to the cross section.

This study has been conducted with the purpose to show that the $^2H(\gamma,\eta)^2H^*$ reaction may provide information which can help to determine the isospin components of the S_{11} electromagnetic transition amplitude and, therefore, to solve the discrepancies mentioned above. The impulse approximation together with a recent fit to the elementary $\gamma+p\rightarrow\eta+p$ transition amplitudes[9] is employed in the calculation. The n-p continuum wave functions are calculated from Reid's soft core potentials.[10] The deuteron breakup accommodates a higher momentum transfer and, thereby, yields a larger total cross section than in the $^2H(\gamma,\eta)^2H$ reaction. It also assures that rescattering effects are negligible compared to single scattering, giving a credit to the employment of impulse approximation. Calculations demonstrate that the cross section is dominated by the S_{11} resonance in the 740 MeV photon laboratory energy region, which is not smeared out by the Fermi motion in the loosely bounded deuteron, in contrast to the case of heavy nuclei targets.[8] Finally, there is a significant difference in the eta cross section when a pure isovector and a pure iso-

scalar elementary amplitude are compared, which can be used to determine the isospin components of the S_{11} resonance.

CHAPTER II

WAVE FUNCTION FOR NEUTRON PROTON ELASTIC SCATTERING

In the neutron-proton center-of-mass coordinate system and, in the space of total spin of n and p, the initial state prior to scattering is

$$|\boldsymbol{k}_i s m_s\rangle = \phi_{\boldsymbol{k}_i s m_s} = (2\pi)^{-3/2} e^{i\boldsymbol{k}_i \cdot \boldsymbol{r}} \chi_{s m_s} , \qquad (2.1)$$

where χ_{sm_s} is the eigenfunction of total spin of n and p. In this equation and the following derivation in this chapter, the units are chosen such that $\hbar$=c=1. The final state after scattering will then be

$$|\boldsymbol{k}_f s' m_s'\rangle = \phi_{\boldsymbol{k}_f s' m_s'} = (2\pi)^{-3/2} e^{i\boldsymbol{k}_f \cdot \boldsymbol{r}} \chi_{s' m_s'} . \qquad (2.2)$$

One may expand $|\boldsymbol{k}_i s m_s\rangle$ as:

$$\phi_{\boldsymbol{k}_i s m_s} = \sqrt{\frac{2}{\pi}} \sum_{lm} i^l Y_{lm}^*(\hat{k}_i)\, Y_{lm}(\hat{r})\, j_l(k_i r)\, \chi_{s m_s}$$

$$= \sqrt{\frac{2}{\pi}} \sum_{lJ} i^l \langle \hat{r} l s m_s | \boldsymbol{Y}^J | \hat{k}_i l s m_s \rangle \chi_{s m_s} j_l(k_i r) , \qquad (2.3)$$

with $\langle \hat{r} l' s' m_s' | \boldsymbol{Y}^J | \hat{k}_i l s m_s \rangle$ defined as

$$\langle \hat{f} l' s' m_s' | \mathbf{Y}^J | \hat{k}_i l s m_s \rangle = \sum_{m'mM} Y_{l'm'}(\hat{f})\, Y^*_{lm}(\hat{k})\, \langle l' m' s' m_s' | JM \rangle \cdot \langle lmsm_s | JM \rangle \ . \qquad (2.4)$$

The S-matrix of the scattering in the c.m. system has the form:

$$\langle b|S|a\rangle = \delta(\mathbf{P}_b)\, \langle \mathbf{k}_f s' m_s' | S | \mathbf{k}_i s m_s \rangle \ , \qquad (2.5)$$

where $|a\rangle$ and $|b\rangle$ are initial and final states, and $\mathbf{P}_b$ is the total momentum in the final state. One can also define a submatrix: $\langle \hat{k}_f s' m_s' | S(k_i) | \hat{k}_i s m_s \rangle$ on the energy shell by

$$\langle \mathbf{k}_f s' m_s' | S | \mathbf{k}_i s m_s \rangle = \frac{1}{\rho_e} \delta [\epsilon(k_f) - \epsilon(k_i)] \cdot \langle \hat{k}_f s' m_s' | S(k_i) | \hat{k}_i s m_s \rangle \ , \qquad (2.6)$$

where $\epsilon(k)$ is the total energy of the reaction and $\rho_e = \frac{k^2}{d\epsilon/dk}_{|k=k_i}$ is the density of states. Correspondingly, the T-matrix can be written in the c.m. system and on the energy shell as $\langle \mathbf{k}_f s' m_s' | T(k_i) | \mathbf{k} s m_s \rangle$ and,

$$\langle \hat{k}_f s' m_s' | T(k_i) | \hat{k}_i s m_s \rangle = \langle \mathbf{k}_f s' m_s' | T | \mathbf{k}_i s m_s \rangle_{|k_f = k_i} \ . \qquad (2.7)$$

The S-matrix and T-matrix are related as

$$\langle \hat{k}_f s' m_s' | S(k_i) | \hat{k}_i s m_s \rangle = \delta_{ss'} \delta_{m_s m_s'} \delta_{\hat{k}_i \hat{k}_f} - 2\pi i \rho_e \cdot \cdot \langle \hat{k}_f s' m_s' | T(k_i) | \hat{k}_i s m_s \rangle . \quad (2.8)$$

The differential cross section for unpolarized beam and target is given by

$$\frac{d\bar{\sigma}}{d\Omega} = \frac{1}{4} \sum_{s' m_s' s m_s} \frac{d\sigma}{d\Omega} (\hat{k}_f s' m_s'; \boldsymbol{k}_i s m_s) , \quad (2.9)$$

where

$$\frac{d\sigma}{d\Omega} (\hat{k}_f s' m_s'; \boldsymbol{k}_i s m_s) = \frac{(2\pi)^4}{v_{rel.}} \rho_e | \langle \hat{k}_f s' m_s' | T(k_i) | \hat{k}_i s m_s \rangle |^2 . \quad (2.10)$$

Resolving the S-matrix into its submatrices for the states of given total angular momentum J with the transformation matrix:

$$\langle \hat{k} s m_s | l m s m_s \rangle = Y_{lm}(\hat{k}) , \quad (2.11)$$

one has

$$\langle \hat{k}_f s' m_s' | S(k_i) | \hat{k}_i s m_s \rangle$$

$$- \sum_{\substack{l' m' J' M' \\ l m J M}} \langle \hat{k}_f s' m_s' | l' m' s' m_s' \rangle \langle l' m' s' m_s' | J' M' \rangle \cdot$$

$$\cdot\langle l's'J'M'|S(k_i)\,|lsJM\rangle\langle lmsm_s|JM\rangle\langle lmsm_s|\hat{k}_i sm_s\rangle \ . \qquad (2.12)$$

Because of conservation of total angular momentum,

$$\langle l's'J'M'|S(k_i)\,|lsJM\rangle = \delta_{JJ'}\delta_{MM'}S^J_{l's'ls}(k_i) \ . \qquad (2.13)$$

Eq. (2.12) can then be written as

$$\langle \hat{k}_f s'm'_s|S(k_i)\,|\hat{k}_i sm_s\rangle = \sum_{l'lJ}\langle \hat{k}_f l's'm'_s|\mathbf{Y}^J|\hat{k}_i lsm_s\rangle \cdot S^J_{l's'ls}(k_i) \ . \qquad (2.14)$$

Similar operation on the T-matrix gives

$$\langle \hat{k}_f s'm'_s|T|\hat{k}_i sm_s\rangle = \sum_{l'lJ}\langle \hat{k}_f l's'm'_s|\mathbf{Y}^J|\hat{k}_i lsm_s\rangle \cdot T^J_{l's'ls}(k_f,k_i) \ , \qquad (2.15)$$

where $T^J_{l's'ls}(k_i,k_i)=T^J_{l's'ls}(k_i)$ on the energy shell with $k_f=k_i$. Here, $S^J_{l's'ls}(k_i)$ and $T^J_{l's'ls}(k_i)$ are related as:

$$S^J_{l's'ls}(k_i) = \delta_{ll'}\delta_{ss'} - 2\pi i\rho_e T^J_{l's'ls}(k_i) \ . \qquad (2.16)$$

The Scattering Wave Equation

The scattering wave function $\Psi^+_{k_i sm_s}$ in the c.m. coor-

dinate system is given by

$$\Psi^{+}_{\boldsymbol{k}_i s m_s}(\boldsymbol{r}) = \phi_{\boldsymbol{k}_i s m_s} + \sum_{s' m_s'} \int \frac{d^3 k' \phi_{\boldsymbol{k}' s' m_s'}}{\epsilon(k) - \epsilon(k') + i\eta} \cdot \langle \boldsymbol{k}' s' m_s' | T | \boldsymbol{k}_i s m_s \rangle \ . \qquad (2.17)$$

With eqs. (2.3), (2.4) and (2.15), $\Psi^{+}_{\boldsymbol{k}_i s m_s}$ is resolved into substates of given total angular momentum J:

$$\Psi^{+}_{\boldsymbol{k}_i s m_s}(\boldsymbol{r}) = \sum_{\substack{l' l J \\ s' m_s'}} \langle \hat{r} l' s' m_s' | \mathcal{Y}^{J} | \hat{k}_i l s m_s \rangle \chi_{s' m_s'} \psi^{+}_{l' s', k_i J l s}(r) \ , \qquad (2.18)$$

where

$$\psi^{+}_{l' s', k_i J l s} = i^{l'} \sqrt{\frac{2}{\pi}} \left[\delta_{l l'} \delta_{s s'} j_l(k_i r) + \int \frac{j_l(k' r)\,(k')^2 dk'}{\epsilon(k_i) - \epsilon(k') + i\eta} T^{J}_{l' s' l s}(k', k_i) \right] , \qquad (2.19)$$

with the asymptotic behavior[11] as:

$$\lim_{r \to \infty} \psi^{+}_{l' s', k_i J l s}(r) = \sqrt{\frac{2}{\pi}}\, i^{l'} \left\{ \delta_{l l'} \delta_{s s'} j_l(k_i r) - \frac{e^{i k_i r}}{k_i r} \left[\pi \rho_e (-i)^{l'} T^{J}_{l' s' l s}(k_i) \right] \right\} , \qquad (2.20a)$$

or

$$\lim_{r\to\infty}\psi^{+}_{l's',k_iJls}(r)=\frac{1}{i\sqrt{2\pi}k_ir}\{-(-1)^{l}\delta_{ll'}\delta_{ss'}e^{-ik_ir}+S^{J}_{l's'ls}e^{ik_ir}\}\ . \quad (2.20b)$$

The wave scattering function $\Psi^{+}_{k_ism_s}$ satisfies Schrödinger equation:

$$(\nabla^2_r+k_i^2-\upsilon)\,\Psi^{+}_{k_ism_s}=0\ , \quad (2.21)$$

where $\upsilon=2m_rV$, $m_r=\frac{m_nm_p}{m_n+m_p}$. V is n-p interaction.

To obtain the equation for the radial wave function $\psi^{+}_{l's',k_iJls}(r)$, one has, from the above equation (2.21), the following expression:

$$\sum_{m_s'}(\chi_{s'm_s'},\int d\Omega_{\hat{k}_i}d\Omega_{\hat{r}}\langle \hat{r}l's'm_s|\mathcal{Y}^{J}|\hat{k}_ilsm_s\rangle^{*}(\nabla^2_r+k_i^2-\upsilon)\,\Psi^{+}_{k_ism_s})=0\ . \quad (2.22)$$

With the expression of $\Psi^{+}_{k_ism_s}$ in eq. (2.18), the definition of eq. (2.4) and orthogonality of Clebsch-Gordan coefficients, the following radial wave equation is obtained:

$$[\frac{1}{r^2}\frac{d}{dr}(r^2\frac{d}{dr})-\frac{l'(l'+1)}{r^2}+k_i^2]\,\psi^+_{l's',k_iJls}(r)$$

$$-\sum_{l''s''} i^{l'-l''}v^J_{l's'l''s''}(r)\,\psi^+_{l''s'',k_iJls}(r)\ , \qquad (2.23)$$

where $v^J_{l's'l''s''}(r)$ is defined as

$$v^J_{l's'l''s''}(r)=i^{l''-l'}\frac{2s+1}{2J+1}\sum_{m_s'm_s''}(\chi_{s'm_s'},\int d\Omega_{\hat{k}_i}d\Omega_{\hat{r}}\langle \hat{r}l's'm_s'|\mathbf{Y}^J|\hat{k}_ilsm_s\rangle^*$$

$$\cdot v\langle \hat{r}l''s''m_s''|\mathbf{Y}^J|\hat{k}_ilsm_s\rangle\chi_{s''m_s''})\ . \qquad (2.24)$$

These coupled differential equations (2.23) should be solved subject to the above asymptotic boundary conditions eqs. (2.20).

Now let us define $R^J_{l's'ls}(r)$ and $U^J_{l's'ls}(r)$ as

$$\psi^+_{l's',k_iJls}(r)=i^{l'}\sqrt{\frac{2}{\pi}}R^J_{l's'ls}(r)=i^{l'}\sqrt{\frac{2}{\pi}}\frac{U^J_{l's'ls}(r)}{r}\ . \qquad (2.25)$$

The equation for $U^J_{l's'ls}(r)$ is then

$$[\frac{d^2}{dr^2}-\frac{l'(l'+1)}{r^2}+k_i^2]\,U^J_{l's'ls}(r)-\sum_{l''s''}v^J_{l's'l''s''}U^J_{l''s''ls}=0\ . \qquad (2.26)$$

The asymptotic behavior of $U^J_{l's'ls}(r)$, following from eq. (2.20b), is given by

$$\lim_{r\to\infty} U^J_{l's'ls}(r) = \frac{1}{2ik_i}\{\delta_{ll'}\delta_{ss'}(-i^{l'})\, e^{-ik_i r} + S^J_{l's'ls}(-i)^{l'} e^{ik_i r}\} . \qquad (2.27)$$

In the asymptotic region where np interaction is negligible one has two linearly independent solutions of the above equation:

$$F_l = k_i r j_l(k_i r) \xrightarrow{r\to\infty} -\frac{i}{2}\left[e^{i(k_i r - \frac{l\pi}{2})} - e^{-i(k_i r - \frac{l\pi}{2})}\right] , \qquad (2.27a)$$

$$G_l = k_i r n_l(k_i r) \xrightarrow{r\to\infty} -\frac{1}{2}\left[e^{i(k_i r - \frac{l\pi}{2})} + e^{-i(k_i r - \frac{l\pi}{2})}\right] , \qquad (2.27b)$$

where j_l and n_l are the spherical Bessel functions. One can rewrite the above asymptotic behavior of $U^J_{l's'ls}(r)$ as:

$$\lim_{r\to\infty} U^J_{l's'ls}(r) = \frac{1}{2k_i}\lim_{r\to\infty}[\delta_{ll'}\delta_{ss'}(F_{l'} - iG_{l'}) + S^J_{l's'ls}(F_{l'} + iG_{l'})] . \qquad (2.28)$$

Now we examine in detail the property of the radial wave equation:

$$\left[\frac{d^2}{dr^2} - \frac{l'(l'+1)}{r^2} + k_i^2\right] U^J_{l's'ls}(r)$$

$$- \sum_{l''s''} v^J_{l's'l''s''}(r)\, U^J_{l''s''ls}(r) . \qquad (2.29)$$

The general form for nucleon-nucleon potential subject to

rotational-invariance, parity and isospin conservation is

$$V = V_c(r) + V_s(r)\,(\vec{\sigma}_1\cdot\vec{\sigma}_2) + V_{LS}(r)\,(\vec{L}\cdot\vec{S}) + V_T[3\,(\vec{\sigma}_1\cdot\hat{r})\,(\vec{\sigma}_2\cdot\hat{r}) - \vec{\sigma}_1\cdot\vec{\sigma}_2] \quad . \quad (2.30)$$

It is easy to demonstrate that

$$[V,\ J^2] = 0 \qquad (2.31a)$$

$$[V,\ J_z] = 0 \qquad (2.31b)$$

$$[V,\ P] = 0 \qquad (2.31c)$$

$$[V,\ S^2] = 0 \qquad (2.31d)$$

where P is parity operator. Here, the Hamiltonian **H** together with J^2, J_z, S^2 and P form a complete set of observables for the two nucleon system. One can have simultaneous eigenfunctions of **H**, J^2, J_z, S^2 and the parity P. Two nucleon spins couple to singlet states (s=0) or triplet states (s=1). So the eigenstates of two nucleon system with well-defined J, M, S and parity P will be the following:

singlet states: $s=0 \quad l=J \quad P=(-1)^J$,

triplet states: $s=1$
$$\begin{cases} l=J & P=(-1)^J & \text{if } J\neq 0 \\ l=J\pm 1 & P=(-1)^{J+1} & \text{if } J\neq 0 \\ l=1 & & \text{if } J=0 \end{cases} .$$

Also from the permutation relations (2.31) and the definition of $v^J_{l's'ls}$, one has that

$$v^J_{l's'ls}=0\ , \tag{2.32}$$

unless $s'=s$ *and* $(-1)^{l'-l}=1$. With the above argument and properties of T-matrix, the following transition scheme between different nucleon-nucleon states (lsJ) is obtained:

One channel scattering:

$$\begin{bmatrix} s=0\ l=J \\ singlet \end{bmatrix} \xrightarrow[transition]{scattering} \begin{bmatrix} s=0\ l=J \\ singlet \end{bmatrix},$$

$$\begin{bmatrix} s=1\ l=J \\ triplet \end{bmatrix} \xrightarrow[transition]{scattering} \begin{bmatrix} s=1\ l=J \\ triplet \end{bmatrix},$$

$$\begin{bmatrix} s=1\ J=0 \\ triplet \end{bmatrix} \xrightarrow[transition]{scattering} \begin{bmatrix} s=1\ J=0 \\ triplet \end{bmatrix}.$$

Examples of one-channel scattering states are $^1S_0$, $^3P_0$, $^1P_1$, $^3P_1$, $^1D_2$, $^3D_2$.

Two channel scattering:

$$\begin{bmatrix} s=1\ l=J+1 \\ triplet \end{bmatrix} \xrightarrow{scattering} \begin{bmatrix} s=1\ l=J+1 \\ triplet \end{bmatrix}$$

$$\begin{bmatrix} s=1\ l=J-1 \\ triplet \end{bmatrix} \xrightarrow[transition]{} \begin{bmatrix} s=1\ l=J-1 \\ triplet \end{bmatrix}.$$

Examples of two-channel scattering states are $^3S_1$-$^3D_1$ and

$^3P_2$-$^3F_2$. Due to the above restrictions on transitions between two-nucleon states (lsJ) arising from the symmetry property of nucleon-nucleon interactions, the radial wave equation (2.26) can be simplified as following:

1. Equations for one-channel scattering:

$$[\frac{d^2}{dr^2}-\frac{l(l+1)}{r^2}+k_i^2]\,U^J_{lsls}-v^J_{lsls}\cdot U^J_{lsls}\,, \qquad (2.33a)$$

where s=0 or 1, l=J; or s=l=1, J=0;

2. Equations for two-channel scattering:

$$[\frac{d^2}{dr^2}-\frac{l(l+1)}{r^2}+k_i^2]\,U^J_{llll}-v^J_{llll}\cdot U^J_{llll}+v^J_{lll'l}\cdot U^J_{l'lll}$$

$$[\frac{d^2}{dr^2}-\frac{l'(l'+1)}{r^2}+k_i^2]\,U^J_{l'lll}-v^J_{l'll'l}\cdot U^J_{l'lll}+v^J_{l'lll}\cdot U^J_{llll}\,, \qquad (2.33b)$$

where s=1, J≠0; l=J+1, l'=J-1; or l=J-1, l'=J+1.

Before discussing solutions of the above radial wave equations, we will first look at diagonalization of the S-matrix. First, the S-matrix is unitary over the physical space spanned by the continuum scattering wave state $\Psi^{\pm}_{\alpha}$, where α represents the scattering channel. Also, time reversal symmetry requires[11] that

$$S^J_{l's'ls}=S^J_{lsl's'}\,.$$

These properties of the S-matrix enable us to write the

$S^J_{l'_s l_s}$ as:

1. One-channel scattering:

$$S^J_{l_s l_s} = e^{2i\delta^J_{l_s}} , \tag{2.34a}$$

2. Two-channel scattering:

$$S^J = \begin{pmatrix} S^J_{J-1,1,J-1,1} & S^J_{J+1,1,J-1,1} \\ S^J_{J-1,1,J+1,1} & S^J_{J+1,1,J+1,1} \end{pmatrix} = \begin{pmatrix} \cos 2\epsilon_J e^{2i\delta_1} & -i\sin 2\epsilon_J e^{i(\delta_1+\delta_2)} \\ -i\sin 2\epsilon_J e^{i(\delta_1+\delta_2)} & \cos 2\epsilon_J e^{2i\delta_2} \end{pmatrix},$$

where phase shift $\delta^J_{l_s}$, δ_1, δ_2 and mixing parameter ϵ_J are all real numbers.

Now we discuss in detail the solution of radial wave equations (3.34). First, the expression of $v^J_{l'_s l''_{s''}}$ will be simplified. According to its definition eq. (2.24),

$$v^J_{l'_s l''_{s''}}(r) = i^{l''-l'} \frac{2s+1}{2J+1} \sum_{m'_s m''_s} (\chi_{s'm'_s} , \int d\Omega_{\hat{k}_i} d\Omega_{\hat{r}} \langle \hat{r} l' s' m'_s | Y^J | \hat{k}_i l s m_s \rangle^* \cdot v \langle \hat{r} l'' s'' m''_s | Y^J | \hat{k}_i l s m_s \rangle \chi_{s'' m''_s}) .$$

By the definition of eq. (3.4) and the orthogonality for spherical harmonics, one reaches

$$v^J_{l'_s l''_{s''}} = i^{l''-l'} \frac{2s+1}{2J+1} \sum_{m'_s m''_s} (\chi_{s'm'_s} , \int d\Omega_{\hat{r}} \sum_{m' m M_1} Y^*_{l'm'}(\hat{r}) \langle l' m' s' m'_s | J M_1 \rangle \cdot$$

$$\cdot\langle lmsm_s|JM_1\rangle\, v \sum_{m''M} Y_{l''m''}(\hat{r})\langle l''m''s''m_s''|JM\rangle\langle lmsm_s|JM\rangle\chi_{s''m_s''}) \quad . \quad (2.35)$$

By defining $Y_{ls}^{JM}=\sum_{mm_s}\langle lmsm_s|JM\rangle Y_{lm}(\hat{r})\chi_{sm_s}$ and realizing that $\langle lmsm_s|JM_1\rangle\langle lmsm_s|JM\rangle=(\langle lmsm_s|JM\rangle)^2\delta_{MM_1}$, one has

$$v_{l's'l''s''}^{J}=i^{l''-l'}\frac{2s+1}{2J+1}\sum_{mM}\langle Y_{l's'}^{JM}|v|Y_{l''s''}^{JM}\rangle\cdot(\langle lmsm_s|JM\rangle)^2 \quad . \quad (2.36)$$

Because the two-nucleon interaction is rotationally invariant and conserves J_z, S^2 and parity P, $\langle Y_{l's'}^{JM}|v|Y_{l''s''}^{JM}\rangle$ is independent of M and

$$\langle Y_{l's'}^{JM}|v|Y_{l''s''}^{JM}\rangle=\delta_{s's''}\delta_{(-1)^{l''-l'},1}\langle Y_{l's'}^{JM}|v|Y_{l''s'}^{JM}\rangle \quad . \quad (2.37)$$

So one can denote $\langle Y_{l's'}^{JM}|v|Y_{l''s''}^{JM}\rangle$ as $V_{l's'l''s''}^{J}$, and has

$$v_{l's'l''s''}^{J}=i^{l''-l'}V_{l's'l''s''}^{J} \quad . \quad (2.38)$$

Finally, by the definition of $u=U_{lsls}^{J}$, $w=i^{l'-l}U_{l'sls}^{J}$ and eq. (2.38), the radial wave equations (2.34a) and (2.34b) become

1. One-channel scattering:

$$[\frac{d^2}{dr^2}-\frac{l(l+1)}{r^2}+k_i^2]\,u=v^J_{lsls}u\,, \qquad (2.39a)$$

where s=0 or 1, l=J; or s=l=1, J=0;

2. Two-channel scattering:

$$[\frac{d^2}{dr^2}-\frac{l(l+1)}{r^2}+k_i^2]\,u=v^J_{llll}\cdot u+v^J_{lll'l}\cdot w$$

$$[\frac{d^2}{dr^2}-\frac{l'(l'+1)}{r^2}+k_i^2]\,w=v^J_{l'll'l}\cdot w+v^J_{l'lll}\cdot u\,, \qquad (2.39b)$$

where s=1, J≠0; l=J+1, l'=J-1 or l=J-1, l'=J+1. In this case $w=-U^J_{l'sls}$. The asymptotic behavior for u and w is

$$\lim_{r\to\infty}u=\frac{1}{2k_i}\lim_{r\to\infty}[(F_l-iG_l)+S^J_{lsls}(F_l+iG_l)]\,, \qquad (2.40a)$$

$$\lim_{r\to\infty}w=\frac{1}{2k_i}\lim_{r\to\infty}(-1)S^J_{l'lll}(F_{l'}+iG_{l'})\,. \qquad (2.40b)$$

Evaluation of Scattering Wave Functions

In this calculation, Reid's soft core potential[10] is employed for V. This potential is given as function of $x=\mu r$ with $\mu=0.7$ fm^{-1}. With the definition $k=k_i/\mu$ and $v^J_{l's'ls}=V^J_{l's'ls}/\mu^2$, eqs. (2.39a) and (2.39b) will change to

1. One-channel scattering:

$$[\frac{d^2}{dx^2}-\frac{l(l+1)}{x^2}+k^2]\,u=v^J_{lsls}u\,, \qquad (2.41a)$$

where s=0 or 1, l=J; or J=0, l=s=1;

2. Two-channel scattering:

$$[\frac{d^2}{dx^2}-\frac{l(l+1)}{x^2}+k^2]\,u=v^J_{lll}\cdot u+v^J_{lll'_1}\cdot w$$

$$[\frac{d^2}{dx^2}-\frac{l'(l'+1)}{x^2}+k^2]\,w=v^J_{l'_1l'_1}\cdot w+v^J_{l'_1ll}\cdot u\,, \qquad (2.41b)$$

where $J\neq 0$, s=1; l=J-1, l'=J+1, or l=J+1, l'=J-1. The asymptotic behavior becomes

$$\lim_{x\to\infty} u=\frac{1}{2k}\lim_{x\to\infty}[(F_l(kx)-iG_l(kx))+S^J_{lsls}(F_l(kx)+iG_l(kx))]\,, \qquad (2.42a)$$

$$\lim_{x\to\infty} w=\frac{1}{2k}\lim_{x\to\infty}(-1)\,S^J_{l'll}(F_{l'}(kx)+iG_{l'}(kx))\,. \qquad (2.42b)$$

The 4th order Runge-Kutta-Gill method is used to solve the above equations numerically. Linearly independent solutions of u and w are generated from the region where $x\approx 0$ (left side) satisfying u=0 and w=0. At very large x (right side), where the two-nucleon interaction becomes negligible, linearly independent solutions of u and w are also generated. By matching the solutions of u and w from both sides according to the continuous condition of u, w,

du/dx and dw/dx, and requiring that the right side solutions satisfy the asymptotic boundary condition of eqs. (2.42a) and (2.42b), one can calculate the radial wave functions $U^J_{l's'ls}$ for different scattering channels and the phase shift parameters are obtained.

The constants employed in this calculation are:

$$m_p = 938.263 \quad MeV,$$

$$m_n = 939.556 \quad MeV,$$

$$m_r = 938.909/2 \; MeV,$$

$$\frac{2m_r}{\mu^2\hbar^2} = \frac{1}{20.32144} \; \frac{1}{MeV}.$$

The calculation of n-p continuum wave functions is tested by comparing the phase shifts and mixing parameters in this calculation to that in Reid's[10] at selected energies. The agreement is almost perfect. However, it should be made clear that T=1 phase shifts have to be calculated from pp scattering in order to make comparison. This has been done by adding the Coulomb potential to the NN interaction. In the asymptotic region the solutions of the corresponding Schrödinger equations are Coulomb wave functions. The asymptotic boundary conditions is still eqs. (2.43a) and (2.43b), but with F_l and G_l understood as

Coulomb wave functions. The phase parameters are still obtained the same way as in the case when only the NN interaction is involved. T=0 phase parameters are still calculated from np scattering.

For the comparison with Reid's[10], the following constants are employed:

$$m_r = 938.903/2 \quad MeV,$$

$$\frac{2m_r}{\mu^2\hbar^2} = \frac{1}{20.32157} \quad \frac{1}{MeV}.$$

When the Coulomb potential is present, ε/x is added to the NN potential $v^J_{l's'ls}$ with

$$\varepsilon/x = 2m_r e^2/\mu^2\hbar^2 r = 0.049602/x.$$

The phase parameters obtained from this calculation and those of Reid's[10] are compared in Tables 1 and 2.

Table 1

Phase Parameters of T=0 Neutron Proton Scattering Channels

E	$\delta(^1P_1$, radians)			$\delta(^3D_2$, radians)		
Lab,MeV	Reid's[10]	This work	A-M[10]	Reid's[10]	This work	A-M[10]
24	-.033	-.033	-.041	.070	.069	.071

Tabel 1-Continued

E	$\delta(^1P_1$, radians)			$\delta(^3D_2$, radians)		
Lab,MeV	Reid's[10]	This work	A-M[10]	Reid's[10]	This work	A-M[10]
48	-.071	-.071	-.072	.169	.169	.169
96	-.190	-.190	-.182	.312	.311	.309
144	-.312	-.312	-.309	.386	.386	.386
208	-.456	-.456	-.463	.431	.431	.433
304	-.633	-.633	-.646	.449	.449	.451
352	-.708	-.708	-.717	.448	.448	.449

E	$\delta(^3S_1$, radians)			δ^3D_1, radians)		
Lab,MeV	Reid's[10]	This work	A-M[10]	Reid's[10]	This work	A-M[10]
24	1.426	1.426	1.443	-.050	-.050	-.051
48	1.105	1.106	1.138	-.115	-.115	-.123
96	.749	.749	.771	-.215	-.215	-.218
144	.521	.521	.513	-.281	-.280	-.272
208	.300	.300	.269	-.340	-.340	-.329
304	.057	.057	.066	-.403	-.403	-.432
352	-.042	-.042	.020	-.431	-.431	-.494

E	$\sin(2\epsilon_1)$		
Lab,MeV	Reid's[10]	This work	A-M[10]
24	.064	.064	-.042
48	.081	.081	-.102
96	.114	.114	-.055
144	.152	.152	.064
208	.203	.203	.212
304	.269	.269	.368
352	.296	.296	.422

Table 2

Phase Parameters of T=1 Neutron Proton Scattering Channels

E	$\delta(^1S_0$, radians)			$\delta(^1D_2$, radians)		
Lab,MeV	Reid's[10]	This work	A-M[10]	Reid's[10]	This work	A-M[10]
24	.862	.862	.868	.011	.011	.012
48	.696	.696	.686	.027	.027	.029
96	.454	.454	.445	.059	.059	.061
144	.277	.276	.278	.089	.089	.088
208	.093	.093	.101	.123	.123	.120
304	-.118	-.118	-.115	.156	.156	.159
352	-.205	-.205	-.206	.164	.164	.176

E	$\delta(^3P_0$, radians)			$\delta(^3P_1$, radians)		
Lab,MeV	Reid's[10]	This work	A-M[10]	Reid's[10]	This work	A-M[10]
24	.141	.140	.122	-.074	-.074	-.074
48	.198	.198	.213	-.133	-.133	-.132
96	.179	.179	.186	-.228	-.228	-.228
144	.105	.105	.099	-.304	-.304	-.306
208	-.012	-.012	-.009	-.386	-.386	-.387
304	-.184	-.184	-.173	-.479	-.479	-.477
352	-.264	-.264	-.273	-.518	-.518	-.514

E	$\delta(^3P_2$, radians)			$\delta(^3F_2$, radians)		
Lab,MeV	Reid's[10]	This work	A-M[10]	Reid's[10]	This work	A-M[10]
24	.038	.039	.039	.002	.002	.002
48	.093	.093	.095	.005	.005	.006
96	.186	.186	.186	.013	.013	.015
144	.243	.242	.241	.018	.018	.020
208	.277	.277	.277	.022	.022	.022
304	.282	.281	.285	.019	.019	.017
352	.274	.273	.278	.014	.014	.014

Table 2-Continued

E	$\sin(2\epsilon_2)$		
Lab,MeV	Reid's[10]	This work	A-M[10]
24	-.026	-.026	-.029
48	-.057	-.057	-.061
96	-.091	-.091	-.094
144	-.103	-.103	-.103
208	-.104	-.104	-.102
304	-.092	-.092	-.098
352	-.085	-.085	-.099

CHAPTER III

ETA PHOTOPRODUCTION FORMALISM

For the reaction $^2H(\gamma,\eta)^2H^*$ with three-body final states, the unpolarized cross section in the center-of-mass coordinate system (ACM) is given by[11]

$$d\sigma=\frac{1}{2(2J_i+1)}\sum_{\lambda m_i m_n m_p}\frac{(2\pi)^4}{v_{rel.}}\int dp_p dp_n dp_\eta \delta(P_b-P_a)|T_{ba}|^2, \qquad (3.1)$$

where the initial and final states are

$$|a\rangle=|\gamma(\lambda,k),{}^2H(J_i m_i)\rangle, \qquad (3.2a)$$

$$|b\rangle=|\eta(k'),np(m_n,m_p,\kappa)\rangle, \qquad (3.2b)$$

$\mathbf{p}_p$, $\mathbf{p}_n$ and $\mathbf{p}_\eta$ are the momentum of proton, neutron and eta in the final states, and, P_a and P_b are the initial and final total four-momenta. The normalization of a plane-wave state is chosen as $|\mathbf{k}\rangle=1/(2\pi)^{3/2}e^{i\mathbf{k}\cdot\mathbf{r}}$. Here and in the following argument throughout this chapter, the units are chosen so that $\hbar=c=1$. After non-relativistic treatment of n-p relative motion, eq. (3.1) becomes

$$d\sigma=\frac{1}{2(2J_i+1)}\sum_{\lambda m_i m_n m_p}\frac{(2\pi)^4}{v_{rel.}}qE_\eta p\mu|T_{ba}|^2 dE_\eta d\Omega_{k'} d\Omega_p, \qquad (3.3)$$

and

$$\frac{d^2\sigma}{dE_\eta d\Omega_{k'}} = \frac{1}{2(2J_i+1)} \frac{(2\pi)^4}{v_{rel.}} qE_\eta p\mu \sum_{\lambda m_i m_n m_p} \int d\Omega_p |T_{ba}|^2 , \qquad (3.4)$$

where q and E_η are the momentum and total energy of outgoing eta, **p** is the relative n-p momentum and μ is the reduced mass of n and p. The T-matrix T_{ba} is on both the energy and momentum shell, which will be assumed in the following argument except when specifically noted otherwise.

Impulse Approximation for the T-matrix

In this reaction, the T-matrix element is

$$T_{ba} = \langle b|T|a\rangle$$

$$= (\psi_b^-, (H-E_a)\chi_a)$$

$$= (\psi_b^-, V\chi_a) , \qquad (3.5)$$

where

$$\chi_a = \frac{1}{(2\pi)^{3/2}} e^{i\mathbf{kr}} \phi_{J_i m_i}(\xi) , \qquad (3.6)$$

$$\psi_b^- = \chi_b + \frac{1}{E_a - H - i\varepsilon} (U+V')\chi_b , \qquad (3.7)$$

and

$$\chi_b = \frac{1}{(2\pi)^{3/2}} e^{ik'\cdot r'} \frac{1}{(2\pi)^{3/2}} e^{ik\cdot\xi'_r} \chi_{m_p} \chi_{m_n} . \qquad (3.8)$$

In these equations, χ_{m_p} and χ_{m_n} are the proton and neutron spins, ξ and ξ' are the deuteron internal coordinates with their spatial parts denoted as ξ_r and ξ'_r respectively, pointing from n to p. V, V' and U are the γN, ηN and NN interaction respectively. The configuration diagram of this reaction is given in Figure 1 below.

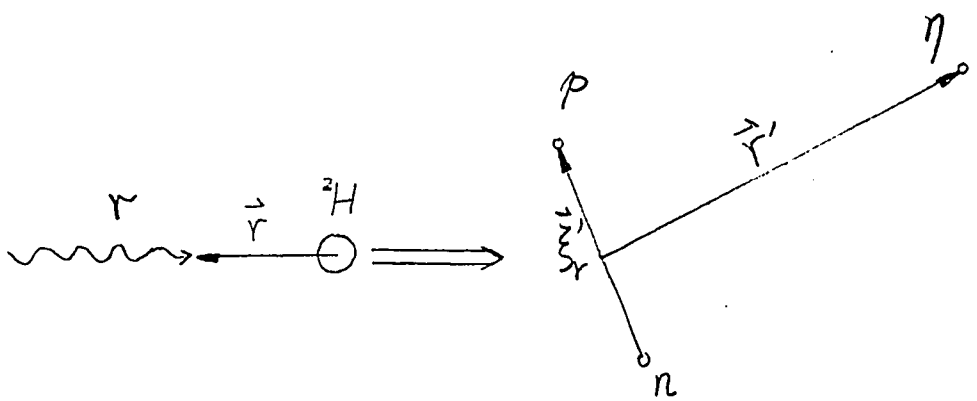

Figure 1. Configuration Diagram of the $^2H(\gamma,\eta)^2H^*$ Reation.

The Hamiltonian can be split in the following way:

$$H = K_a + V = K_b + V' + U , \qquad (3.9)$$

together with the definition:

$$K_a = K_\gamma + K_d \,, \tag{3.10}$$

$$K_b = K_p + K_n + K_\eta \,, \tag{3.11}$$

where the k's are kinetic energy operators. Rewriting ψ_b^- in eq. (3.6) as

$$\psi_b^- = \chi_b + \frac{1}{E_a - K_b - U - i\varepsilon} U\chi_b + \frac{1}{E_a - H - i\varepsilon}(U+V')\chi_b - \frac{1}{E_a - K_b - U - i\varepsilon} U\chi_b \,, \tag{3.12}$$

and defining

$$\phi_b^- = \chi_b + \frac{1}{E_a - K_b - U - i\varepsilon} U\chi_b \,, \tag{3.13}$$

one reaches

$$\psi_b^- = \phi_b^- + \frac{1}{E_a - H - i\varepsilon} V'\phi_b^- \,. \tag{3.14}$$

So with eq. (3.5) and (3.10), the T-matrix element can be written as

$$T_{ba} = (\phi_b^-,\ (V + V'\frac{1}{E_a - H + i\varepsilon} V)\chi_a) \,. \tag{3.15}$$

In the impulse approximation, η is produced either from the proton or from the neutron. One also can assume that the η interacts only with the nucleon it is produced

from. If an on-shell approximation is made for both the γN vertex and the other nucleon (please refer to Figure 2.), the above T-matrix element can be finally given as

$$T_{ba} = (\phi_b^-, \ (T_p + T_n)\chi_a) \ , \tag{3.16}$$

where both T_p and T_n have the form of

$$V + V' \frac{1}{W - H_o + i\varepsilon} V, \tag{3.17}$$

W is the total energy of γ and the struck nucleon in ACM and, $H_o = K_\gamma + K_N + V$. In the spirit of the impulse approximation, T_p is related somehow to the T-matrix of elementary process $\gamma + p \to \eta + p$. So it is necessary to study this elementary reaction first.

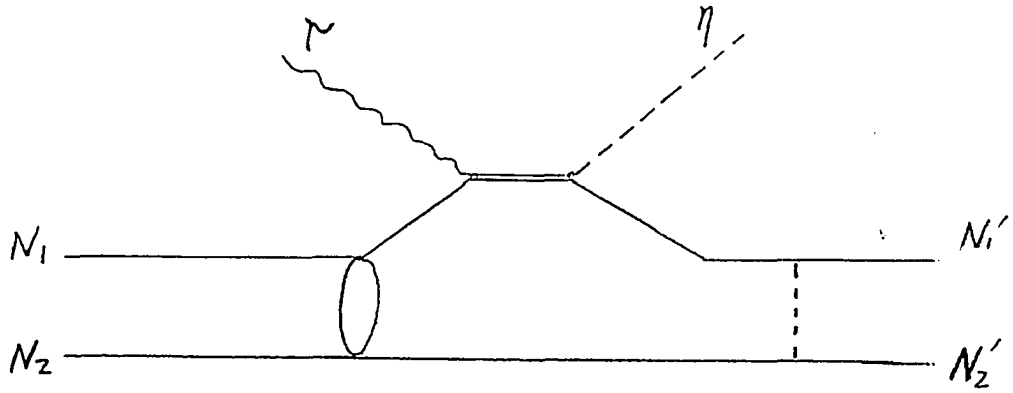

Figure 2. The Corresponding Feynmann Diagram of This Calculation.

In the center-of-mass frame of the reaction $\gamma+p\rightarrow\eta+p$, the T-matrix element is $\langle\eta(\boldsymbol{k}_c'),\ p(m_s')\,|T_c|\gamma(\boldsymbol{k}_c,\lambda),\ p(m_s)\rangle$. Here λ is the photon polarization, m_s and m_s' are the proton spin orientations. All of them are quantized along the direction of $\boldsymbol{k}_c$. Here and in the following argument, all subscript and superscript c indicate the quantities in the γN center-of-mass frame (2CM) unless otherwise stated. The T_c operator is

$$T_c=V_c+V_c'\frac{1}{E^c-H^c+i\varepsilon}V_c\,, \tag{3.18}$$

where E^c and H^c is the total energy and the Hamiltonian of this elementary reaction. A general discussion[11] using rotational and gauge invariance gives, under the transverse gauge, the general form of the above T-matrix element as

$$\langle\boldsymbol{k}_c';\ \tfrac{1}{2}m_s'|T_c|(\boldsymbol{k}_c,\lambda)\,;\ \tfrac{1}{2}m_s\rangle=\langle\tfrac{1}{2}m_s'|\mathcal{F}|\tfrac{1}{2}m_s\rangle\,, \tag{3.19}$$

with $\mathcal{F}$ given by

$$\mathcal{F}=\mathcal{F}_1(\sigma\cdot\hat{\epsilon})+\mathcal{F}_2(i\sigma\cdot\hat{k}_c')\,(\sigma\cdot\hat{\epsilon}\times\hat{k}_c)+\mathcal{F}_3(\sigma\cdot\hat{k}_c\hat{k}_c'\cdot\hat{\epsilon})+\mathcal{F}_4(\sigma\cdot\hat{k}_c'\hat{k}_c'\cdot\hat{\epsilon})\,, \tag{3.20}$$

where $\hat{\epsilon}$ is photon polarization vector and $\mathcal{F}_i$ are functions of magnititude of $\boldsymbol{k}_c$, $\boldsymbol{k}_c'$ and the angle θ_c between them. The

$\mathcal{F}$ can also be written as

$$\mathcal{F}=(\mathcal{F}_1-\mathcal{F}_2\cos\theta_c)\,\sigma\cdot\hat{e}+i\mathcal{F}_2\hat{e}\cdot(\hat{k}_c\times\hat{k}'_c)+(\mathcal{F}_2+\mathcal{F}_3)\,(\sigma\cdot\hat{k}_c\hat{k}'_c\hat{e})+\mathcal{F}_4(\sigma\cdot\hat{k}'_c\hat{k}'_c\hat{e})\ . \tag{3.21}$$

By writing the matrix element of T_c as

$$\langle \boldsymbol{k}'_a;\tfrac{1}{2}m'_s|T_c|(\boldsymbol{k}_a,\hat{e})\,;\tfrac{1}{2}m_s\rangle=(\frac{1}{(2\pi)^{3/2}}e^{i\boldsymbol{k}'_a\cdot\boldsymbol{r}'_a}\chi_{m'_s}\,,$$

$$T_c(\hat{e},\frac{1}{(2\pi)^{3/2}}e^{i\boldsymbol{k}_a\cdot\boldsymbol{r}_a}\chi_{m_s}))\ , \tag{3.22}$$

and applying standard approximation $\boldsymbol{r}'_c=\boldsymbol{r}_a$, one has

$$\langle \boldsymbol{k}'_a;\tfrac{1}{2}m'_s|T_c|(\boldsymbol{k}_a,\hat{e})\,;\tfrac{1}{2}m_s\rangle=(\frac{1}{(2\pi)^{3/2}}e^{i\boldsymbol{k}'_a\cdot\boldsymbol{r}_a}\chi_{m'_s}\,,$$

$$T_c(\hat{e},\frac{1}{(2\pi)^{3/2}}e^{i\boldsymbol{k}_a\cdot\boldsymbol{r}_a}\chi_{m_s}))\ . \tag{3.23}$$

Now it is assumed that photon and nucleon interact only when they are very close together. Then one can apply a zero-range approximation to T_c: $T_c=v_c\delta(\boldsymbol{r}_a)$ which yields

$$\langle \boldsymbol{k}'_a;\tfrac{1}{2}m'_s|T_c|(\boldsymbol{k}_a,\hat{e})\,;\tfrac{1}{2}m_s\rangle=\langle\tfrac{1}{2}m'_s|\frac{1}{(2\pi)^3}v_c|\tfrac{1}{2}m_s\rangle\ . \tag{3.24}$$

By comparing this equation with eq. (3.19), one reaches

$$v_c=(2\pi)^3\mathcal{F}, \tag{3.25}$$

a constant. The elementary amplitude F_c, which satisfies

$$\left(\frac{d\sigma}{d\Omega}\right)_c = \frac{k_c'}{k_c}|<\frac{1}{2}m_s'|F_c|\frac{1}{2}m_s>|^2 , \tag{3.26}$$

is related to $\mathcal{F}$ as

$$F_c = (2\pi)^2 \bar{W}_c \mathcal{F}, \tag{3.27}$$

with $\bar{W}_c = \frac{(E_\gamma^c E_N^c E_N^{c'} E_\eta^c)^{1/2}}{E^c}$ and, has the same form as $\mathcal{F}$:

$$F = F_1(\sigma\cdot\hat{\epsilon}) + F_2(i\sigma\cdot\hat{k}_c')(\sigma\cdot\hat{\epsilon}\times\hat{k}_c) + F_3(\sigma\cdot\hat{k}_c\hat{k}_c'\hat{\epsilon}) + F_4(\sigma\cdot\hat{k}_c'\hat{k}_c'\hat{\epsilon})$$

$$= (F_1 - F_2\cos\theta_c)\sigma\cdot\hat{\epsilon} + iF_2\,\hat{\epsilon}\cdot(\hat{k}_c\times\hat{k}_c') + (F_2+F_3)(\sigma\cdot\hat{k}_c\hat{k}_c'\hat{\epsilon}) + F_4(\sigma\cdot\hat{k}_c'\hat{k}_c'\hat{\epsilon}) . \tag{3.28}$$

With the above elementary amplitude, v_c can also be given as

$$v_c = (2\pi)^3 \frac{1}{(2\pi)^2} \frac{1}{\bar{W}_c} F_c . \tag{3.29}$$

Now go back to the T-matrix element eq. (3.16) in ACM and rewrite it as following:

$$T_{ba} = (\phi_b^-(\xi', r'), (T_p + T_n)\frac{1}{(2\pi)^{3/2}} e^{ikr}\phi_{J_i m_i}(\xi)) . \tag{3.30}$$

Application of standard approximation:

$$\boldsymbol{r}'=\frac{m_d}{m_{np}}\boldsymbol{r}, \quad \boldsymbol{\xi}'=\boldsymbol{\xi}\,, \tag{3.31}$$

where m_d is the deuteron mass and m_{np} is the mass of np system in the final state, leads to

$$T_{ba}=(\phi_b^-(\xi,\frac{m_d}{m_{np}}\boldsymbol{r})\,,\ (T_p+T_n)\frac{1}{(2\pi)^{3/2}}e^{i\boldsymbol{k}\cdot\boldsymbol{r}}\phi_{J_1m_1}(\xi))\,. \tag{3.32}$$

Again zero-range approximation is made to T_p and T_n:

$$T_p=v_p\delta(\boldsymbol{r}-\frac{1}{2}\xi_r)\,, \tag{3.33}$$

$$T_n=v_n\delta(\boldsymbol{r}+\frac{1}{2}\xi_r)\,. \tag{3.34}$$

Then, by the impulse approximation, v_p should be the counter part of v_c in the ACM system, which should be obtained by transforming from v_c as a T-matrix:

$$v_p=\nu v_c\,, \qquad \nu=\left(\frac{E_\gamma{}^cE_N{}^cE_N{}^{c'}E_\eta{}^c}{E_\gamma\,E_N\,E_N'\,E_\eta}\right)^{1/2}. \tag{2.35}$$

This step means that on-shell approximation has been made dynamically for both the ηN vertex and the other nucleon

(please refer to Figure 2). Using eq. (3.29), v_p can be written as

$$v_p = (2\pi)^3 \frac{1}{(2\pi)^2} v \frac{1}{\bar{W}_c} F_c^p . \tag{3.36}$$

Here F_c in eq. (3.29) is denoted as F_c^p to indicate that it comes from the reaction $\gamma+p\rightarrow\eta+p$. Similarly, v_n can be given as

$$v_n = (2\pi)^3 \frac{1}{(2\pi)^2} v \frac{1}{\bar{W}_c} F_c^n . \tag{3.37}$$

However, v_n must be obtained from eta photoproduction from nuclear targets. In this calculation, F_c^n is assumed to be proportional to F_c^p. With all the above argument, the T-matrix element of eq. (3.15) now becomes

$$T_{ba} = (\phi_b^-(\xi, \frac{1}{2}\frac{m_d}{m_{np}}\xi_r), v_p \frac{1}{(2\pi)^{3/2}} e^{i\frac{1}{2}k\cdot\xi_r}\phi_{J_i m_i}(\xi))$$

$$+ (\phi_b^-(\xi, -\frac{1}{2}\frac{m_d}{m_{np}}\xi_r), v_n \frac{1}{(2\pi)^{3/2}} e^{-i\frac{1}{2}k\cdot\xi_r}\phi_{J_i m_i}(\xi)) , \tag{3.38}$$

with v_p and v_n given above.

Before calculating the cross section using the above

T-matrix element, the expression of $\phi_b^-(\xi', \boldsymbol{r}')$ has to be figured out.

Time Reversed State ϕ_b^- and Resolution of the Cross Section

By the definition of eq. (3.13), ϕ_b^- is given by

$$\phi_b^- = \chi_b + \frac{1}{E_a - K_p - K_n - K_\eta - U - i\varepsilon} U\chi_b \,. \tag{3.39}$$

Making non-relativistic approximation for K_p, K_n, K_η and the motion of n, p and η in the final state $|b\rangle$, and realizing that U is the interaction between nucleons only, one reaches

$$\phi_b^- = \left(|\kappa, m_p m_n\rangle + \frac{1}{E(\kappa) - H_{np} - i\varepsilon} |\kappa, m_p m_n\rangle\right) \frac{1}{(2\pi)^{3/2}} e^{i\boldsymbol{k}'\cdot\boldsymbol{r}} \,, \tag{3.40}$$

where $E(\kappa)$ and H_{np} are the kinetic energy and non-relativistic Hamiltonian of n-p relative motion. Here and in the following argument in this section, the coordinates ξ' and $\mathbf{r}'$ of the final state $|b\rangle$ are denoted as ξ and $\mathbf{r}$ respectively to avoid confusion. Denoted as $\psi^-_{\kappa, m_p m_n}$,

$|\kappa, m_p m_n\rangle + \frac{1}{E(\kappa) - H_{np} - i\varepsilon} |\kappa, m_p m_n\rangle$ is the time reversed state of

$$\psi^{/+}_{-\kappa,-m_p-m_n} = |-\kappa,-m_p-m_n\rangle^{/} + \frac{1}{E(\kappa)-H_{np}+i\varepsilon}|-\kappa,-m_p-m_n\rangle^{/}, \qquad (3.41)$$

where $|-\kappa,-m_p-m_n\rangle^{/}$ is the time reserved state of $|\kappa,m_pm_n\rangle$, which can be expressed as

$$|-\kappa,-m_p-m_n\rangle^{/} = \frac{1}{(2\pi)^{3/2}} e^{-i\kappa\cdot\xi_r}(-1)^{m_p}(-1)^{m_n}|\tfrac{1}{2}-m_p\rangle|\tfrac{1}{2}-m_n\rangle$$

$$= (-1)^{m_p+m_n}\sum_{sm_s}\langle\tfrac{1}{2}-m_p\tfrac{1}{2}-m_n|sm_s\rangle\frac{1}{(2\pi)^{3/2}}e^{-i\kappa\cdot\xi_r}\chi_{sm_s}, \qquad (3.42)$$

where χ_{sm_s} is the wave function for total spin of n and p. Here, the definition and convention of time reversal operation is taken from Ref. 11, and H_{np} is assumed time reversal invariant.

Following the derivation from eq. (2.17) to eq. (2.18) in Chapter II, and using the definition of eq. (2.4) and eq. (2.25) , one reaches

$$\psi^{/+}_{-\kappa,-m_p-m_n} = (-1)^{m_p+m_n}\sum_{l's'lsJ}\sum_{m'_sm_sm'mM}\langle\tfrac{1}{2}-m_p\tfrac{1}{2}-m_n|sm_s\rangle\langle l'm's'm'_s|JM\rangle$$

$$\cdot\langle lmsm_s|JM\rangle Y_{l'm'}(\hat{\xi}_r)\,Y^*_{lm}(-\hat{\kappa})\,\chi_{s'm'_s}\,i^{l'}\sqrt{\frac{2}{\pi}}\;R^J_{l's'ls}(\kappa,\xi_r)\ . \qquad (3.43)$$

Now, by operating with the time reversal operator T on both sides of the above equation, ψ^{-}_{κ,m_pm_n} can be expressed as

$$\psi^{-}_{\kappa,m_p m_n} = T\psi^{l+}_{-\kappa,-m_p-m_n}$$

$$= (-1)^{m_p+m_n} \sum_{l's'lsJ} \sum_{m'_s m_s m' m M} \sum_{m'_p m'_n} \langle \tfrac{1}{2} -m_p \tfrac{1}{2} -m_n | sm_s \rangle \langle \tfrac{1}{2} m'_p \tfrac{1}{2} m'_n | s'm'_s \rangle \cdot$$

$$\cdot \langle l'm's'm'_s | JM \rangle \langle lmsm_s | JM \rangle (-1)^{m'} Y_{l'-m'}(\hat{\xi}_r) Y_{lm}(-\hat{\kappa}) (-i)^{l'} \sqrt{\frac{2}{\pi}} \cdot$$

$$\cdot R^{J*}_{l's'ls}(\kappa, \xi_r) (-1)^{m'_p} \chi_{-m'_p} (-1)^{m'_n} \chi_{-m'_n} . \qquad (3.44)$$

By changing the sign of all m's in eq. (3.44) and using the symmetry properties of Clesch-Gorden coefficients, $\psi^{-}_{\kappa,m_p m_n}$ is finally given by

$$\psi^{-}_{\kappa,m_p m_n} = \sum_{l's'lsJ} \sum_{mm_s M} \sqrt{\frac{2}{\pi}} \langle \tfrac{1}{2} m_p \tfrac{1}{2} m_n | sm_s \rangle \langle lmsm_s | JM \rangle Y^*_{lm}(\hat{\kappa}) \cdot$$

$$\cdot \phi^{JM}_{l's'ls}(\kappa, \xi) , \qquad (3.45)$$

where $\phi^{JM}_{l's'ls}(\kappa, \xi)$ is defined by

$$\phi^{JM}_{l's'ls}(\kappa, \xi) = \sum_{m'_p m'_n m'_s m'} \langle \tfrac{1}{2} m'_p \tfrac{1}{2} m'_n | s'm'_s \rangle \langle l'm's'm'_s | JM \rangle \cdot$$

$$\cdot \chi_{m'_p} \chi_{m'_n} Y_{l'm'}(\hat{\xi}_r) i^{l'} R^{J*}_{l's'ls}(\kappa, \xi_r) . \qquad (3.46)$$

Notice that $\phi^{JM}_{l's'ls}(\kappa, \xi)$ is an eigenstate of L^2, S^2, J^2 and J_z.

In conclusion, ϕ^{-}_{b} is given by

$$\phi_b^-(\xi,r) = \frac{1}{(2\pi)^{3/2}} e^{ik'\cdot r} \sum_{l's'lsJ} \sum_{mm_sM} \sqrt{\frac{2}{\pi}} \langle \frac{1}{2} m_p \frac{1}{2} m_n | s m_s \rangle \cdot$$

$$\cdot \langle lm s m_s | JM \rangle Y_{lm}^*(\hat{k}) \cdot \phi_{l's'ls}^{JM}(\kappa,\xi) \ , \qquad (3.47)$$

with $\phi_{l's'ls}^{JM}(\kappa,\xi)$ defined as above.

Now, with all the preparation above, the cross section eq. (3.4) is ready to be evaluated. However, one will find that it can be resolved into partial cross sections as following.

From eq. (3.38), (3.40), the T-matrix element T_{ba} can be expressed explicitly as

$$T_{ba} = \left(\frac{1}{(2\pi)^{3/2}} e^{i\frac{1}{2}\frac{m_d}{m_{np}} k'\cdot\xi_x} \psi^-_{\kappa, m_p m_n}(\xi) , \ v_p \frac{1}{(2\pi)^{3/2}} e^{i\frac{1}{2} k\cdot\xi_x} \phi_{J_i m_i}(\xi) \right)$$

$$+ \left(\frac{1}{(2\pi)^{3/2}} e^{-i\frac{1}{2}\frac{m_d}{m_{np}} k'\cdot\xi_x} \psi^-_{\kappa, m_p m_n}(\xi) , \ v_n \frac{1}{(2\pi)^{3/2}} e^{-i\frac{1}{2} k\cdot\xi_x} \phi_{J_i m_i}(\xi) \right) . \qquad (3.48)$$

The argument in the last section indicates that v_p and v_n are just summation of some tensor operators which do not contain derivative operators with respect to spatial coordinates. Defining $Q = \frac{1}{2}(k - \frac{m_d}{m_{np}} k')$, eq. (3.48) becomes

$$T_{ba}=\frac{1}{(2\pi)^3}\left(\psi^{-}_{\kappa,m_p m_n}(\xi)\,,\ \sum_{J_x m_x}{}'\left(e^{i\varrho\xi_x}(v_p)^{J_x}_{m_x}+e^{-i\varrho\xi_x}(v_n)^{J_x}_{m_x}\right)\phi_{J_i m_i}(\xi)\right),$$

(3.49)

where Σ' indicates the summation over just restricted pairs of (J_x, m_x). Using eq. (3.45), the orthogonalities and symmetry properties of Clesch-Gordan coefficients, and the following identities and definitions:

$$e^{i\varrho\xi_x}=\sum_{LM}4\pi i^{L}j_L(\varrho\xi_x)\,Y_{LM}(\hat{\xi}_x)\,Y^{*}_{LM}(\hat{\varrho})\,,$$

$$Y_{LM}(\hat{\xi}_x)\cdot(v_p+(-1)^{L}v_n)^{J_x}_{m_x}=\sum_{J_B m_B}\langle LMJ_x m_x|J_B m_B\rangle\cdot$$

$$\cdot\left[Y_L(\hat{\xi}_x)\otimes(v_p+(-1)^{L}v_n)^{J_x}\right]^{J_B}_{m_B},$$

$$\langle\phi^{JM}_{l'S'lS}(\kappa,\xi)\,|\left[Y_L(\hat{\xi}_x)\otimes(v_p+(-1)^{L}v_n)^{J_x}\right]^{J_B}_{m_B}j_L(\varrho\xi_x)\,i^{L}|\phi_{J_i m_i}(\xi)\rangle$$

$$=\langle J_i m_i J_B m_B|JM\rangle\langle\phi^{J}_{l'S'lS}||\left[Y_L(\hat{\xi}_x)\otimes(v_p+(-1)^{L}v_n)^{J_x}\right]^{J_B}_{m_B}j_L i^{L}||\phi_{J_i}\rangle_R$$

$$=\langle J_i m_i J_B m_B|JM\rangle\tau^{LJ_xJ_BJ_i}_{lsl'S'J}\,,$$

one reaches

$$\langle|T_{ba}|^2\rangle=\sum_{m_i m_n m_p}\int d\Omega_p|T_{ba}|^2$$

$$=\frac{16}{(2\pi)^5}\sum_{\substack{J_x m_x\\ \bar{J}_x\bar{m}_x}}{}'\sum_{\substack{LM\\ \bar{L}\bar{M}}}\sum_{\substack{lsJl'S'\\ \bar{l}'\bar{S}'J_B m_B}}Y^{*}_{LM}(\hat{\varrho})\,Y_{\bar{L}\bar{M}}(\hat{\varrho})\cdot$$

$$\cdot \frac{[J]}{[J_B]} \langle LMJ_x m_x | J_B m_B \rangle \langle \bar{L}\bar{M}\bar{J}_x \bar{m}_x | J_B m_B \rangle \cdot$$

$$\cdot \tau^{LJ_x J_B J_i}_{ls l' s' J} \tau^{\bar{L}\bar{J}_x J_B J_i *}_{ls \bar{l}' \bar{s}' J} , \qquad (3.50)$$

where [J]=2J+1, etc. On the other hand, by defining

$$T_{Jls} = \left(\frac{1}{(2\pi)^{3/2}} e^{i \frac{m_d}{m_{np}} k' \cdot r} \sum_{l's'} \phi^{JM}_{l's'ls}(\xi) , \; \left(V_p \delta \left(r - \frac{1}{2} \xi_r \right) \right. \right.$$

$$\left. \left. + V_n \delta \left(r + \frac{1}{2} \xi_r \right) \right) \frac{1}{(2\pi)^{3/2}} e^{ikr} \phi_{J_i m_i}(\xi) \right) , \qquad (3.51)$$

and following the same precedure as above, one also has

$$\sum_{m_i M} |T_{Jls}|^2 = \frac{4}{(2\pi)^4} \sum_{J_x m_x \bar{J}_x \bar{m}_x} \sum_{LML\bar{M}} \sum_{\substack{l's'\bar{l}'\bar{s}' \\ J_B m_B}} Y^*_{LM}(\hat{Q}) \, Y_{\bar{L}\bar{M}}(\hat{Q}) \cdot$$

$$\cdot \frac{[J]}{[J_B]} \langle LMJ_x m_x | J_B m_B \rangle \langle \bar{L}\bar{M}\bar{J}_x \bar{m}_x | J_B m_B \rangle \cdot$$

$$\cdot \tau^{LJ_x J_B J_i}_{ls l' s' J} \tau^{\bar{L}\bar{J}_x J_B J_i *}_{ls \bar{l}' \bar{s}' J} . \qquad (3.52)$$

From eq.(3.4), (3.51) and (3.52) together with the definition:

$$\left(\frac{d\sigma}{d\Omega} \right)_{lsJ} = \frac{1}{2[J_i]} \frac{(2\pi)^4}{v_{rel.}} \frac{q E_\eta E_{np}}{E^A} \sum_{\lambda m_i M} |T_{lsJ}|^2 , \qquad (3.53)$$

one can finally express cross section (3.4) as

$$\frac{d^2\sigma}{dE_\eta d\Omega_{k'}} = \frac{pE^A m_N}{\pi E_{np}} \sum_{lsJ} \left(\frac{d\sigma}{d\Omega}\right)_{lsJ}, \qquad (3.54)$$

where E^A is the total energy of this reaction and E_{np} is the total energy of final np system in ACM.

Evaluation of Cross Sections

From the argument of the last section, the cross section of reaction $^2H(\gamma,\eta)^2H^*$ is resolved into the contributions from each final np state of $(l_f s_f J_f)$. Once this partial cross section is calculated for each $(l_f s_f J_f)$ n-p final state, the cross section for this reaction can be obtained from eq. (3.54). Here and in the following derivation, $(l_f s_f J_f)$ is used instead of (lsJ) to represent np states after reaction in order to avoid confusion. Noticing that

$$\frac{1}{v_{rel.}} = \frac{E_\gamma E_d}{E^A p_\gamma}, \qquad (3.55)$$

where E_γ and p_γ are the photon energy and momentum and E_d is the deuteron energy before reaction, $(\frac{d\sigma}{d\Omega})_{l_f s_f J_f}$ becomes

$$\left(\frac{d\sigma}{d\Omega}\right)_{l_f s_f J_f} = (2\pi)^4 \frac{k}{k'} \frac{E_\gamma E_d E_\eta E_{np}}{(E^A)^2} \frac{1}{2[J_i]} \sum_{\lambda m_i m_f} |T_{l_f s_f J_f}|^2 . \qquad (3.56)$$

From eq. (3.36), (3.37), (3.51) and the definition of Q in eq. (3.49), the matrix element $T_{l_f s_f J_f}$ can be written as

$$T_{l_f s_f J_f} = \frac{1}{(2\pi)^2} \nu \frac{1}{\bar{W}_c} (1+(-1)^{l_f+s_f+s_i}\gamma_o) \cdot$$

$$\cdot(\phi_{J_f m_f}(\xi)\, e^{-i\mathbf{Q}\mathbf{r}},\ F_c^p \phi_{J_i m_i}(\xi)) \ , \qquad (3.57)$$

where $\sum_{l's'} \phi^{J_f m_f}_{l's' l_f s_f}(\kappa,\xi)$ has been denoted as $\phi_{J_f m_f}(\xi)$; and $\mathbf{r}$ has been used to denote the spatial part of np internal coordinate ξ, pointing from n to p. $\gamma_o = F_c^p/F_c^n$. The sign $(-1)^{l_f+s_f+s_i}$ comes from the interchange of n-p internal coordinates. One should notice the selectivities on (l's') from Chapter II. From eqs. (3.56) and (3.57) one finally has

$$\left(\frac{d\sigma}{d\Omega}\right)_{l_f s_f J_f} = [1+(-1)^{l_f+s_f+s_i}\gamma_o]^2 \frac{k}{k'} \frac{(E^c)^2 E_d E_{np}}{(E^A)^2 E_N E'_N} \frac{1}{2[J_i]} \cdot$$

$$\cdot \sum_{\lambda m_i m_f} |(\phi_{J_f m_f}(\xi)\, e^{-i\mathbf{Q}\mathbf{r}},\ F_c^p \phi_{J_i m_i}(\xi))|^2 \ . \qquad (3.58)$$

Now the only thing left is to compute the quantity:

$$\sum_{\lambda m_i m_f} |(\phi_{J_f m_f}(\xi)\, e^{-i\mathbf{Q}\mathbf{r}},\ F_c^p \phi_{J_i m_i}(\xi))|^2 \ .$$

It can be written as in the following by using the expression (3.28),

$$\sum_{\lambda m_i m_f} |(\phi_{J_f m_f}(\xi)\, e^{-i\mathbf{Q}\cdot\mathbf{r}},\ F_c^p \phi_{J_i m_i}(\xi))|^2$$

$$-\sum_{\lambda m_i m_f} \Big|\int \phi^*_{J_f m_f}(\xi)\, e^{i\mathbf{Q}\cdot\mathbf{r}} [(F_1 - F_2\cos\theta_c)\,\sigma_\lambda + iF_2(\hat{k}_c\times\hat{k}_c')_\lambda$$

$$+(F_2+F_3)\,\sigma_o(\hat{k}_c')_\lambda + F_4(\sigma\cdot\hat{k}_c')(\hat{k}_c')_\lambda]\,\phi_{J_i m_i}(\xi)\, d\xi\Big|^2 . \qquad (3.59)$$

Denoting the four terms in the above equation as #1, #2, #3 and #4 separately, the expansion of the above $|\ |^2$ will yield the following terms: #1⊗#1, #1⊗#2, #1⊗#3, #1⊗#4, #2⊗#2, #2⊗#3, #2⊗#4, #3⊗#3, #3⊗#4, #4⊗#4 and their complex conjugates. Each of these terms has to be evaluated separately. Before doing this, some preparation is needed.

The following identities and definitions are used in the derivation:

(a) The expansion of $e^{i\mathbf{q}\cdot\mathbf{r}}$ in terms of spherical harmonics:

$$e^{i\mathbf{q}\cdot\mathbf{r}} = 4\pi\sum_{lm} i^l j_l(qr)\, Y^*_{lm}(\hat{q})\, Y_{lm}(\hat{r}) .$$

(b) The coupling of two spherical harmonics:

$$Y_{l_1 m_1}(\hat{q})\, Y_{l_2 m_2}(\hat{q}) = \sum_{LM} \frac{\hat{l}_1\hat{l}_2}{\sqrt{4\pi}\hat{L}} \langle l_1 m_1 l_2 m_2 | LM\rangle \langle l_1 0\, l_2 0 | L0\rangle\, Y_{LM}(\hat{q})$$

$$-\sum_{LM}\frac{\hat{l}_1\hat{l}_2\hat{L}}{\sqrt{4\pi}}(-1)^M\begin{pmatrix}l_1 l_2 L\\0\ 0\ 0\end{pmatrix}\begin{pmatrix}l_1 l_2 L\\m_1 m_2 M\end{pmatrix}Y_{L-M}(\hat{Q})\ .$$

(c) Orthogonalities and symmetry properties of Clebsch-Gordan, 3j and 6j coefficients.

(d)

$$\sum_{\mu_1\mu_2\mu_3}(-1)^{l_1+l_2+l_3+\mu_1+\mu_2+\mu_3}\begin{pmatrix}j_1 l_2\ l_3\\m_1\ \mu_2-\mu_3\end{pmatrix}\begin{pmatrix}l_1 j_2 l_3\\-\mu_1 m_2\ \mu_3\end{pmatrix}\begin{pmatrix}l_1\ l_2 j_3\\\mu_1-\mu_2 m_3\end{pmatrix}$$

$$=\begin{pmatrix}j_1 j_2 j_3\\m_1 m_2 m_3\end{pmatrix}\begin{Bmatrix}j_1 j_2 j_3\\l_1 l_2 l_3\end{Bmatrix},$$

from which one frequently-used identity is obtained:

(e)

$$\sum_{mm'M}\begin{pmatrix}l\,l'L\\-m\,m'M\end{pmatrix}\langle lm1\lambda|IM_I\rangle\langle l'm'1\lambda'|IM_I\rangle(-1)^m$$

$$=(-1)^{L-I+\lambda'}[I]\begin{pmatrix}1\ L1\\-\lambda' M\lambda\end{pmatrix}\begin{Bmatrix}1L1\\l\,I\,l'\end{Bmatrix}$$

for integer l.

(f) Reduced matrix of irreducible tensor operator:

$$\langle j'm'|X^J_M|jm\rangle=\langle jmJM|j'm'\rangle\frac{1}{\hat{j}}\langle j'\|X^J\|j\rangle\ .$$

(g) Coupling of two tensor operators:

$$T^{k_1}_{q_1} U^{k_1}_{q_1} = \sum_{KQ} \langle k_1 q_1 k_2 q_2 | KQ \rangle \, [T^{k_1} \otimes U^{k_2}]^{K}_{Q} .$$

Another thing which is frequently encountered in the derivation is the matrix element: $\langle \phi_{J_f m_f} | X^{J}_{m_J} j_l(Qr) | \phi_{J_i m_i} \rangle$ where $X^{J}_{m_J}$ is either $Y_{lm}(\hat{r})$ or $[Y_l \otimes \sigma]^{J}_{m_J}$. Realizing that the operator X will only act on the proton, the above matrix element can be expanded as

$$\begin{aligned}
&\langle \phi_{J_f m_f} | X^{J}_{m_J} j_l(Qr) | \phi_{J_i m_i} \rangle \\
&= \langle \sum_{l's'} R^{*}_{l's'} i^{l'} [Y_{l'} \otimes (\tfrac{1}{2}\tfrac{1}{2})^{s'}]^{J_f}_{m_f} | X^{J}_{m_J} j_l(Qr) | \sum_{l_i} R_{l_i s_i} [Y_{l_i} \otimes (\tfrac{1}{2}\tfrac{1}{2})^{s_i}]^{J_i}_{m_i} \rangle \\
&= \sum_{l's'j'} \sum_{l_i s_i j_i} \int (-i)^{l'} R_{l's'} R_{l_i s_i} j_l(Qr) \, r^2 dr \, (-1)^{l_i + l' + J_f + J_i + 2} \hat{j'} \hat{j} \hat{s'} \hat{s}_i \cdot \\
&\cdot \begin{Bmatrix} l' & \frac{1}{2} & j' \\ \frac{1}{2} & J_f & s' \end{Bmatrix} \begin{Bmatrix} l_i & \frac{1}{2} & j \\ \frac{1}{2} & J_i & s_i \end{Bmatrix} \langle [(Y_{l'} \otimes \tfrac{1}{2})^{j'} \otimes \tfrac{1}{2}]^{J_f}_{m_f} | X^{J}_{m_J} | [(Y_{l_i} \otimes \tfrac{1}{2})^{j} \otimes \tfrac{1}{2}]^{J_i}_{m_i} \rangle ,
\end{aligned} \tag{3.60}$$

where $R_{l's'}$ stands for radial wave function $R^{J_f}_{l's' l_f s_f}(\kappa, r)$ in eq. (3.46) and, $R_{l_i s_i}$ is the radial wave function of deuteron. In the total spin wave function, coupling order is $s_p \otimes s_n$. The selectivity of $(l_i s_i J_i)$ is l_i=1,2, s_i=J_i=1. One should refer to Chapter II for the selectivity of

$(l's')$. Remembering that X only acts on the proton, and together with identities and definition (c), (d) and (f), one has

$$\langle [(Y_{l'}\otimes\tfrac{1}{2})^{j'}\otimes\tfrac{1}{2}]^{J_f}_{m_f}| X^J_{m_J} | [(Y_{l_i}\otimes\tfrac{1}{2})^{j}\otimes\tfrac{1}{2}]^{J_i}_{m_i}\rangle$$

$$= (-1)^{j'-\frac{3}{2}+2m_f+2m_i+J_i-J}\frac{\hat{J}_i\hat{j}'}{\hat{J}}\begin{Bmatrix} j' & J_f & \frac{1}{2} \\ J_i & j & J \end{Bmatrix}\langle J_i m_i J m_J | J_f m_f\rangle \cdot$$

$$\cdot\langle (Y_{l'}\otimes\tfrac{1}{2})^{j'}\| X^J \|(Y_{l_i}\otimes\tfrac{1}{2})^{j}\rangle . \qquad (3.61)$$

Combining eq. (3.60) and (3.61), and appreviate index $(l's'j')$ as α and $(l_i s_i j)$ as β, one finally has

$$\langle \phi_{J_f}\| X^J_{m_J} j_l(Qr)\|\phi_{J_i}\rangle$$

$$-\sum_{\alpha\beta} A_{\alpha\beta}\hat{j}'\frac{1}{\hat{J}}\int (-i)^{l'} R_{l's'} R_{l_i s_i} j_l r^2 dr \langle (Y_{l'}\otimes\tfrac{1}{2})^{j'}\| X^J \|(Y_{l_i}\otimes\tfrac{1}{2})^{j}\rangle \qquad (3.62)$$

where

$$A_{\alpha\beta} = (-1)^{l'+l_i+J_f+J+j'+\frac{1}{2}}\hat{s}'\hat{s}_i\hat{j}\hat{j}'\hat{J}_i\hat{J}\begin{Bmatrix} j' & J_f & \frac{1}{2} \\ J_i & j & J \end{Bmatrix}\cdot$$

$$\cdot\begin{Bmatrix} l' & \frac{1}{2} & j' \\ \frac{1}{2} & J_f & s' \end{Bmatrix}\begin{Bmatrix} l_i & \frac{1}{2} & j \\ \frac{1}{2} & J_i & s_i \end{Bmatrix} . \qquad (3.63)$$

The following quantities defined for $X^J_{m_J}$-$Y_{lm}(\hat{r})$ and $X^J_{m_J}$-$[Y_l \otimes \sigma]^J_{m_J}$ are also used in this derivation:

(h)

$$T^l_{\alpha\beta} = i^l \hat{l} A_{\alpha\beta} \hat{j}' \frac{1}{\hat{J}} \int (-1)^{l'} R_{l's'} R_{l_i s_i} j_l r^2 dr \cdot$$

$$\cdot \langle (Y_{l'} \otimes \frac{1}{2})^{j'} \| Y_l \| (Y_{l_i} \otimes \frac{1}{2})^{j_i} \rangle .$$

(i)

$$\tau^{lJ}_{\alpha\beta} = i^l \hat{l} A_{\alpha\beta} \hat{j}' \frac{1}{\hat{J}} \int (-1)^{l'} R_{l's'} R_{l_i s_i} j_l r^2 dr \cdot$$

$$\cdot \langle (Y_{l'} \otimes \frac{1}{2})^{j'} \| [Y_l \otimes \sigma]^J \| (Y_{l_i} \otimes \frac{1}{2})^{j_i} \rangle .$$

Please refer to Appendix A for the formula of the reduced matrix elements $\langle (Y_{l'} \otimes \frac{1}{2})^{j'} \| X^J \| (Y_{l_i} \otimes \frac{1}{2})^{j_i} \rangle$ for both $X^J_{m_J}$-$Y_{lm}(\hat{r})$ and $X^J_{m_J}$-$[Y_l \otimes \sigma]^J_{m_J}$.

Now, with all the above definitions and identities (a) through (i) plus eq. (3.62) and (3.63), all the terms in the expansion of eq. (3.59) are derived to yield the following results:

$$\#1\otimes\#1 = 4\pi|F_1 - F_2\cos\theta_c|^2 \sum_{\substack{l_1 l_2 J \\ L=0,2}} \sum_{\alpha_1\beta_1\alpha_2\beta_2} (-1)^{J+1} \frac{2[J_f]}{[J]} \langle 1\,1\,1\,-1|L0\rangle \cdot$$

$$\cdot \langle l_1 0 l_2 0|L0\rangle \begin{Bmatrix} 1 & L & 1 \\ l_1 & J & l_2 \end{Bmatrix} \tau^{l_1 J}_{\alpha_1\beta_1} \left(\tau^{l_2 J}_{\alpha_2\beta_2}\right)^* P_L(\cos\theta_Q) \ . \qquad (3.64)$$

$$\#1\otimes\#3 = -2Re\left[4\pi (F_1 - F_2\cos\theta_c)(F_2 + F_3)^* \sum_{\substack{l_1 l_2 J \\ \alpha_1\beta_1\alpha_2\beta_2}} (-1)^J \sqrt{\frac{3}{2}} \frac{[J_f]}{[J]} \cdot \right.$$

$$\left. \cdot \langle l_1 0 l_2 0|2\,0\rangle \begin{Bmatrix} 1 & 2 & 1 \\ l_1 & J & l_2 \end{Bmatrix} \tau^{l_1 J}_{\alpha_1\beta_1} \left(\tau^{l_2 J}_{\alpha_2\beta_2}\right)^* \cos\theta_Q \sin\theta_Q \sin\theta_c \right] \ . \qquad (3.65)$$

$$\#1\otimes\#4 = -2Re\left[(4\pi)^2 (F_1 - F_2\cos\theta_c) F_4^* \sum_{\substack{l_1 l_2 J \\ LMI=0,2}} \sum_{\alpha_1\beta_1\alpha_2\beta_2} (-1)^J \frac{[J_f]}{\hat{L}\hat{I}[J]} \cdot \right.$$

$$\cdot \langle 1\,0\,1\,0|I0\rangle \langle l_1 0 l_2 0|L0\rangle \begin{Bmatrix} 1 & L & 1 \\ l_1 & J & l_2 \end{Bmatrix} \tau^{l_1 J}_{\alpha_1\beta_1} \left(\tau^{l_2 J}_{\alpha_2\beta_2}\right)^* \cdot$$

$$\cdot \left(\delta_{IL}(-1)^M Y_{L-M}(\hat{Q})\, Y_{LM}(\hat{k}'_c) - (-1)^M \langle 1\,0\,1\,-M|L-M\rangle \cdot \right.$$

$$\left. \cdot \langle 1\,0\,1\,-M|I-M\rangle Y_{L-M}(\hat{Q})\, Y_{IM}(\hat{k}'_c) \right] \ . \qquad (3.66)$$

$$\#2\otimes\#2 = 4\pi|F_2|^2 \sin^2\theta_c \sum_{l\alpha_1\beta_1\alpha_2\beta_2} \frac{[J_f]}{[I]^2} T^l_{\alpha_1\beta_1} T^{l*}_{\alpha_2\beta_2} \qquad (3.67)$$

$$\#3\otimes\#3-4\pi|F_2+F_3|^2\sin^2\theta_c\sum_{\substack{l_1l_2J\\L=0,2}}\sum_{\alpha_1\beta_1\alpha_2\beta_2}(-1)^J\frac{[J_f]}{[J]}\langle 1010|L0\rangle\cdot$$

$$\cdot\langle l_1 0 l_2 0|L0\rangle\begin{Bmatrix}1 & L & 1\\ l_1 & J & l_2\end{Bmatrix}\tau^{l_1J}_{\alpha_1\beta_1}\left(\tau^{l_2J}_{\alpha_2\beta_2}\right)^* P_L(\hat{Q}) \quad . \tag{3.68}$$

$$\#3\otimes\#4-2Re[(4\pi)^2(F_2+F_3)F_4^*\sin^2\theta_c\sum_{\substack{l_1l_2J\\L=0,2}}\sum_{\alpha_1\beta_1\alpha_2\beta_2}(-1)^{L+J+1}\frac{[J_f]}{3[J]}\cdot$$

$$\cdot\langle l_1 0 l_2 0|L0\rangle\begin{Bmatrix}1 & L & 1\\ l_1 & J & l_2\end{Bmatrix}\tau^{l_1J}_{\alpha_1\beta_1}\left(\tau^{l_2J}_{\alpha_2\beta_2}\right)^*\cdot$$

$$\cdot\left(\sum_{M=-1}^{1}\langle 1-MLM|10\rangle Y_{L-M}(\hat{Q})\,Y_{1M}(\hat{k}_c')\right)] \quad . \tag{3.69}$$

$$\#4\otimes\#4-(4\pi)^2|F_4|^2\sin^2\theta_c\sum_{\substack{l_1l_2J\\L=0,2}}\sum_{\alpha_1\beta_1\alpha_2\beta_2}(-1)^J\frac{[J_f]}{[L]\cdot[J]}\langle 1010|L0\rangle\cdot$$

$$\cdot\langle l_1 0 l_2 0|L0\rangle\begin{Bmatrix}1 & L & 1\\ l_1 & J & l_2\end{Bmatrix}\tau^{l_1J}_{\alpha_1\beta_1}\left(\tau^{l_2J}_{\alpha_2\beta_2}\right)^*\left(\sum_M(-1)^M Y_{L-M}(\hat{Q})\,Y_{L-M}(\hat{k}_c')\right) \quad . \tag{3.70}$$

The other terms #1⊗#2=#2⊗#3=#2⊗#4=0. In the above expressions, θ_Q is the angle between $\boldsymbol{Q}$ vector and $\boldsymbol{k}$ vector. The z-axis has been chosen in the direction of $\boldsymbol{k}$; P_L is the Lth Legenda polynomial.

Finally,

$$\sum_{\lambda m_i m_f} |(\phi_{J_f m_f}(\xi)\, e^{-i\mathbf{Q}\cdot\mathbf{r}},\ F_c^p \phi_{J_i m_i}(\xi))|^2$$

$$= (\#1\otimes\#1) + (\#1\otimes\#3) + (\#1\otimes\#4) + (\#2\otimes\#2)$$

$$+ (\#3\otimes\#3) + (\#3\otimes\#4) + (\#4\otimes\#4)\ . \qquad (3.71)$$

With eqs. (3.54), (3.58), (3.59), (3.64) through (3.71) and definitions and identities (a) through (i), the cross section (3.4) of this reaction $^2H(\gamma,\eta)^2H^*$ is ready to evaluate.

The Elementary Amplitudes and Forward Angle Approximation

The elementary amplitudes F_i (i=1,2,3,4) are taken from the most recent fit[9] to the elementary $\gamma+p\rightarrow\eta+p$ reaction. It uses the Cutkosky resonances[12] which are more reliable than those used in earlier Hick's fit.[13] In Cutkosky resonances, the S_{11} resonance is peaked at 1510 MeV. Because the threshold of the $^2H(\gamma,\eta)^2H^*$ reaction corresponds a γN center-of-mass energy of E^c=1438 MeV which is much lower than the E^c=1488 MeV threshold of the elementary $\gamma+p\rightarrow\eta+p$ reaction, some model is needed to evaluate the elementary amplitudes for the E^c energy below 1488 MeV. When E^c is smaller than 1490 MeV, this calculation simply freezes the resonance widths and

penetration factors of the Tabakin's fit[9] at their 1490 MeV value, and lets the denominator $(E^c-E_r+i\Gamma/2)$ carry the only energy dependence.

From eq. (3.28), one will notice that the F_c^p operator has to be made as a function of ACM variables. However, how to define k_c and k_c' from ACM variables remains ambiguous. So some approximations have been made in this calculation. First, the F_i is evaluated from γN c.m. (2CM) energy E^c at θ_c=0 degrees (forward angle approximation). Second, the scattering angle θ_c in the 2cm frame is set to be equal to the scattering angle θ_η in the ACM. The second approximation makes $\hat{k}_c'=\hat{k}'$ ($\hat{k}_c=\hat{k}$ anyway). Then eq. (3.28) becomes

$$F=F_1(\sigma\cdot\hat{\epsilon})+F_2(i\sigma\cdot\hat{k}')(\sigma\cdot\hat{\epsilon}\times\hat{k})+F_3(\sigma\cdot\hat{k}\hat{k}'\cdot\hat{\epsilon})+F_4(\sigma\cdot\hat{k}'\hat{k}'\cdot\hat{\epsilon})$$

This second approximation is chosen because at forward angles, where large yield occurs, the difference between $\hat{k}'$ and $\hat{k}_c'$ is expected to be small except for some "flip over" effects at photon laboratory energy close to ACM threshold (632 MeV) and for large enough n-p relative kinetic energy (please see the following argument).

The above approximations mean that this calculation is

only accurate at zero degrees. However, angular distribution is still presented in the result. In order to estimate the effect of these approximations, one can choose some other reasonable prescription for determining F_c^p from ACM variables.

To estimate the effect of the second approximation made above, cross sections are also calculated by Lorentz transforming θ_c from θ_η. This choice is made in order to keep consistent with the impulse and on-shell approximation used in the first section of this chapter. It means ignoring the influence from the other nucleon kinematically. The comparison between the second approximation and the Lorentz transforming method is shown in Figures 3 and 4, where the angular distribution and dependence of the cross section on n-p relative kinetic energy for both T=1 and T=0 final states are plotted. At 650 MeV photon laboratory energy, the Lorentz transforming moves the peak of angular distribution from zero to about 12 degrees, and produces an increase by about 10-20%. The "flip over" effect (at θ_η=0 degrees, the Lorentz transformed θ_c becomes 180 degrees) is also seen in Figure 4 at that photon energy. However, at 700 MeV photon energy the Lorentz transforming produces an difference in angular distribution which is smaller than 5% and, out to 54 degrees keeps the similar dependence of the cross section on n-p relative kinetic energy, only produces

about 10% increase. Obviously, the higher the photon laboratory energy, the smaller the above difference, and the more reliable the second approximation.

For the effect of the first approximation, one may want to refer to Ref. 8.

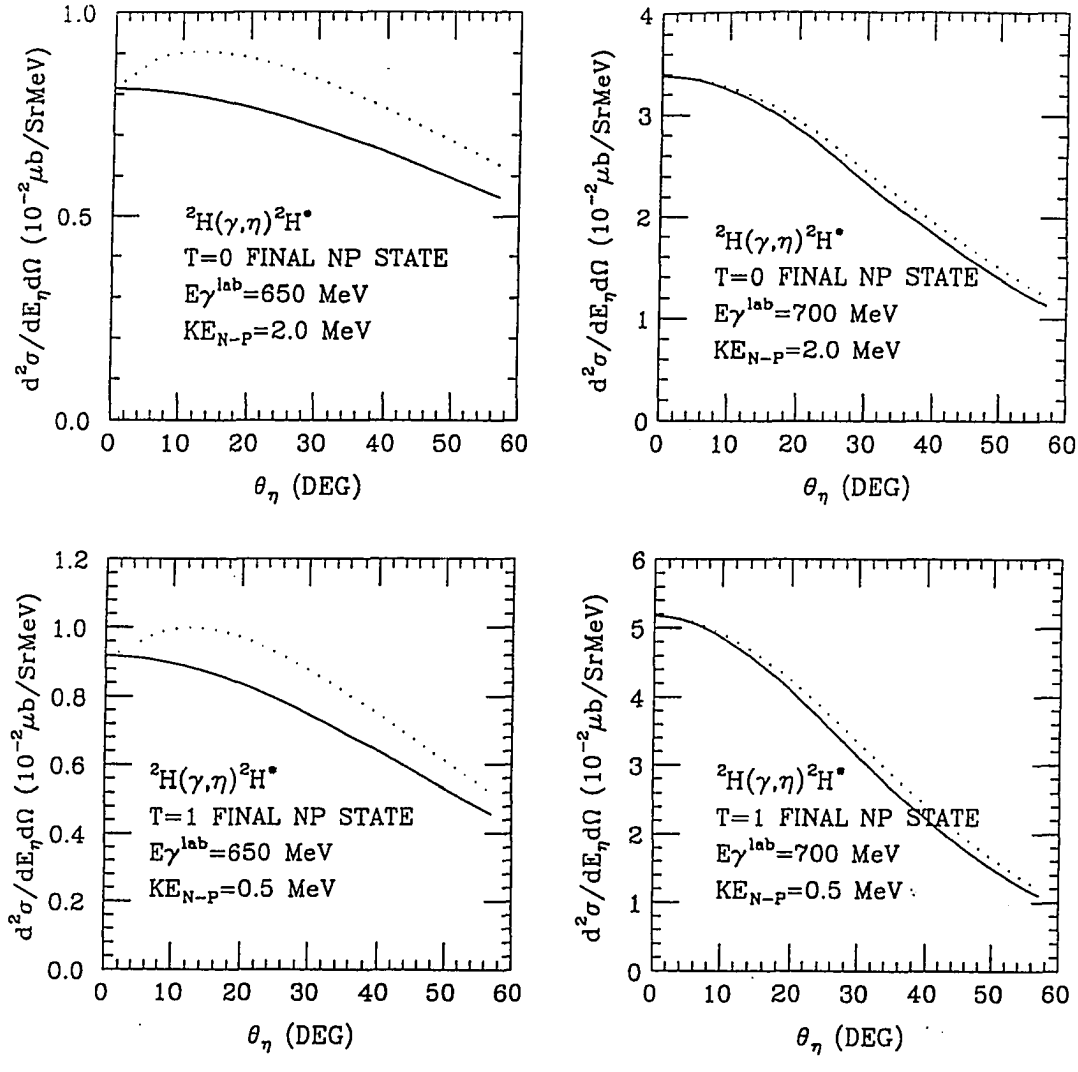

Figure 3. Angular Distributions at Selected KE_{N-P} Values for Both T=1 and T=0 Final States. The Dotted Curves are with Lorentz Transformed θ_c.

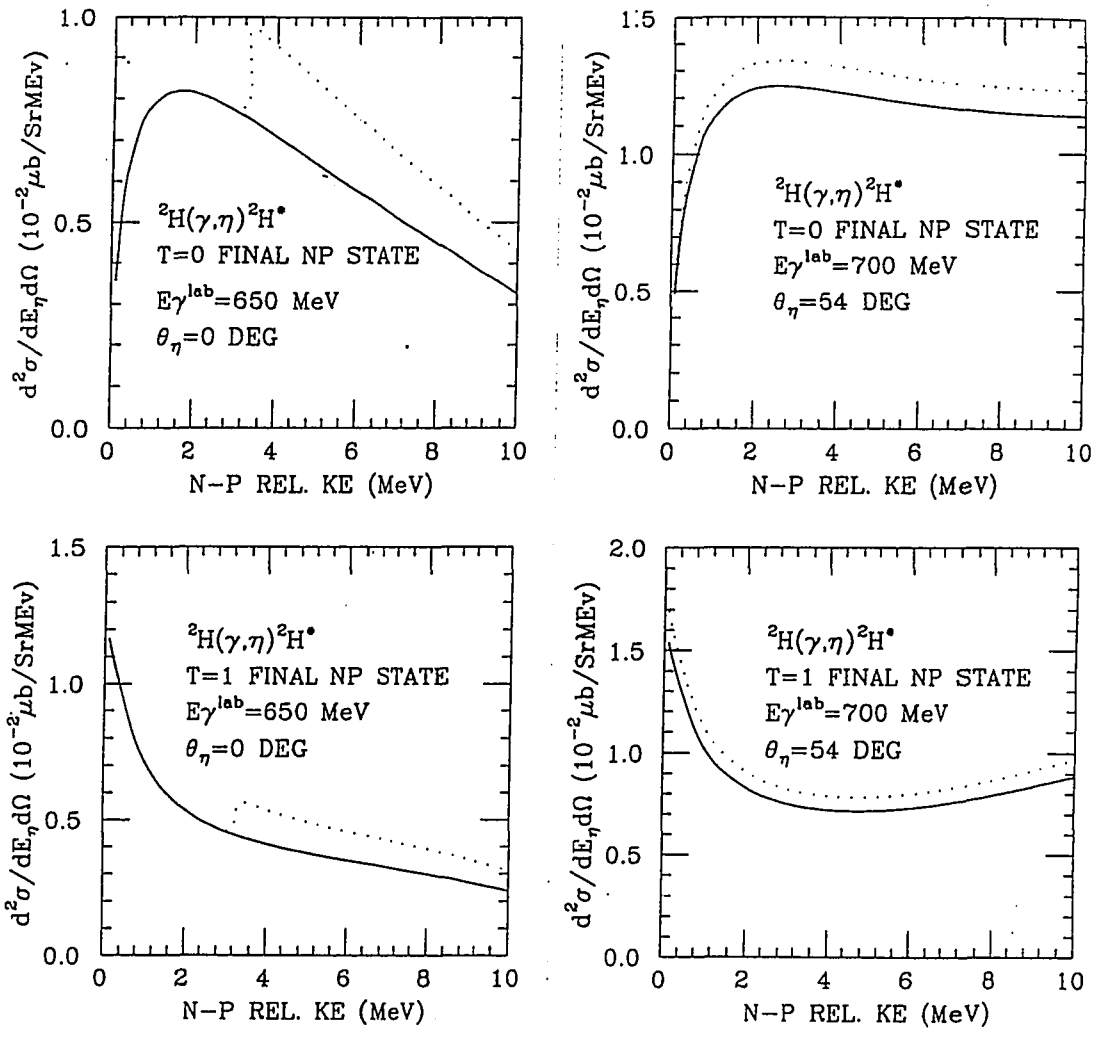

Figure 4. The T=0 and T=1 Cross Sections at Selected Eta Angles as Functions of n-p Relative Kinetic Energy. The Dotted Curves are With Lorentz Transforming θ_c from θ_η.

CHAPTER IV

RESULTS

The double differential cross section $d^2\sigma/dE_\eta d\Omega$ of this reaction $^2H(\gamma,\eta)^2H^*$ depends on the incident photon energy, the outgoing eta energy and angle. The energy of emitted eta meson is uniquely determined by the n-p final relative kinetic energy at a given incident photon energy. So in this work, the cross section has been given as a function of incident photon energy, n-p relative kinetic energy in the final state and outgoing eta angle. All the cross sections are calculated with Fermi-averaging the elementary amplitude except commented otherwise.

It is instructive to see an overview of the above dependence of the cross section. Shown in Figures 5 through 10 are cross sections, for both T=0 and T=1 final states, as functions of the n-p relative kinetic energy KE_{N-P} and the eta angles θ_η. In each of these six graphs, contour lines are plotted at KE_{N-P} of 2, 6, 10 MeV and then in step size of 10 MeV up to its maximum value allowed (e.g., 97 MeV at photon lab energy of 760 MeV), and also for eta angles from 0 to 57 degrees. In Figures 11 and 12, T=0 and T=1 cross sections are also given as functions of θ_η and KE_{N-P}, but confined within 0 to 10 MeV of KE_{N-P}. By comparing

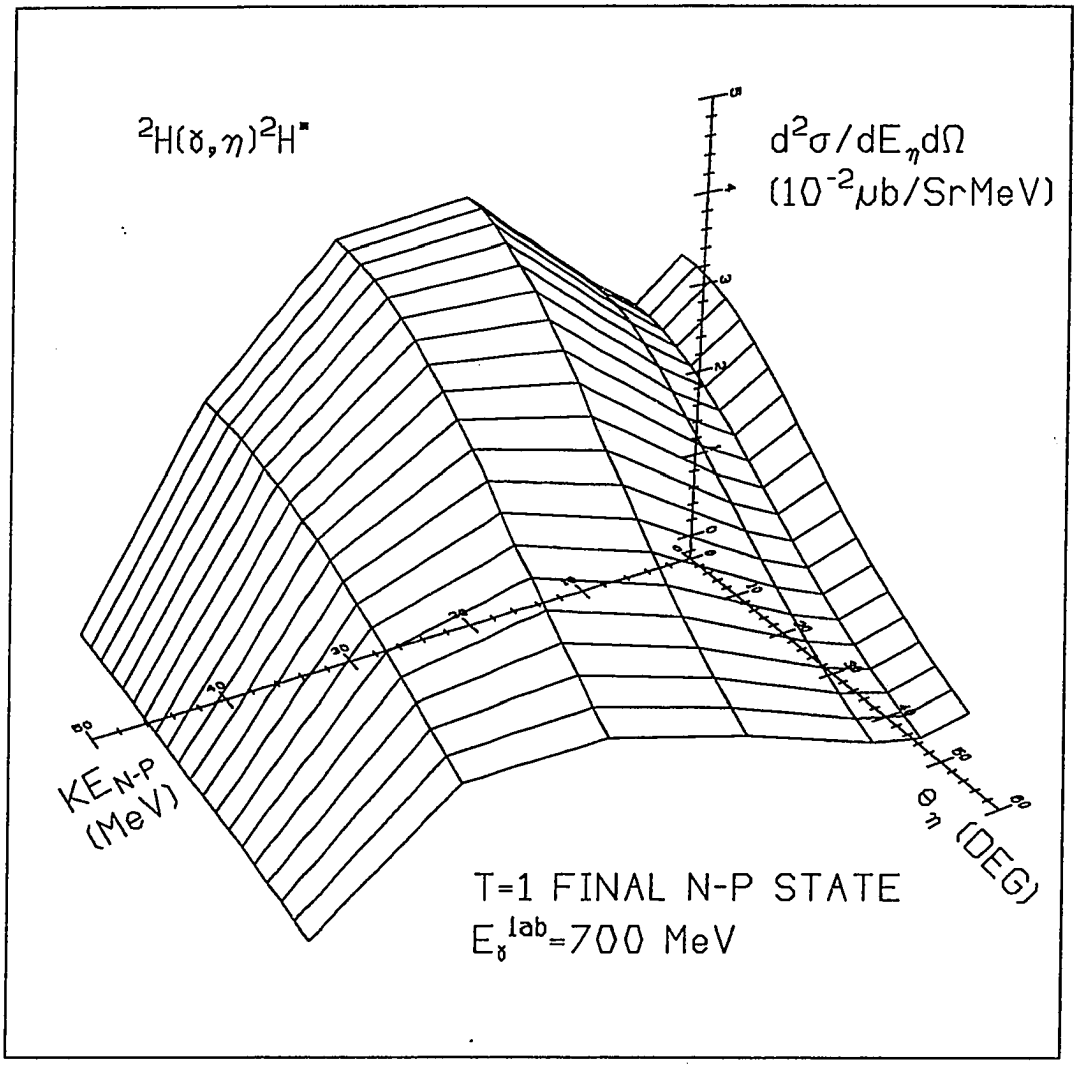

Figure 5. The T=1 Cross Section as a Function of Eta Angle and n-p Relative Kinetic Energy at E_γ^{lab}=700 *MeV*.

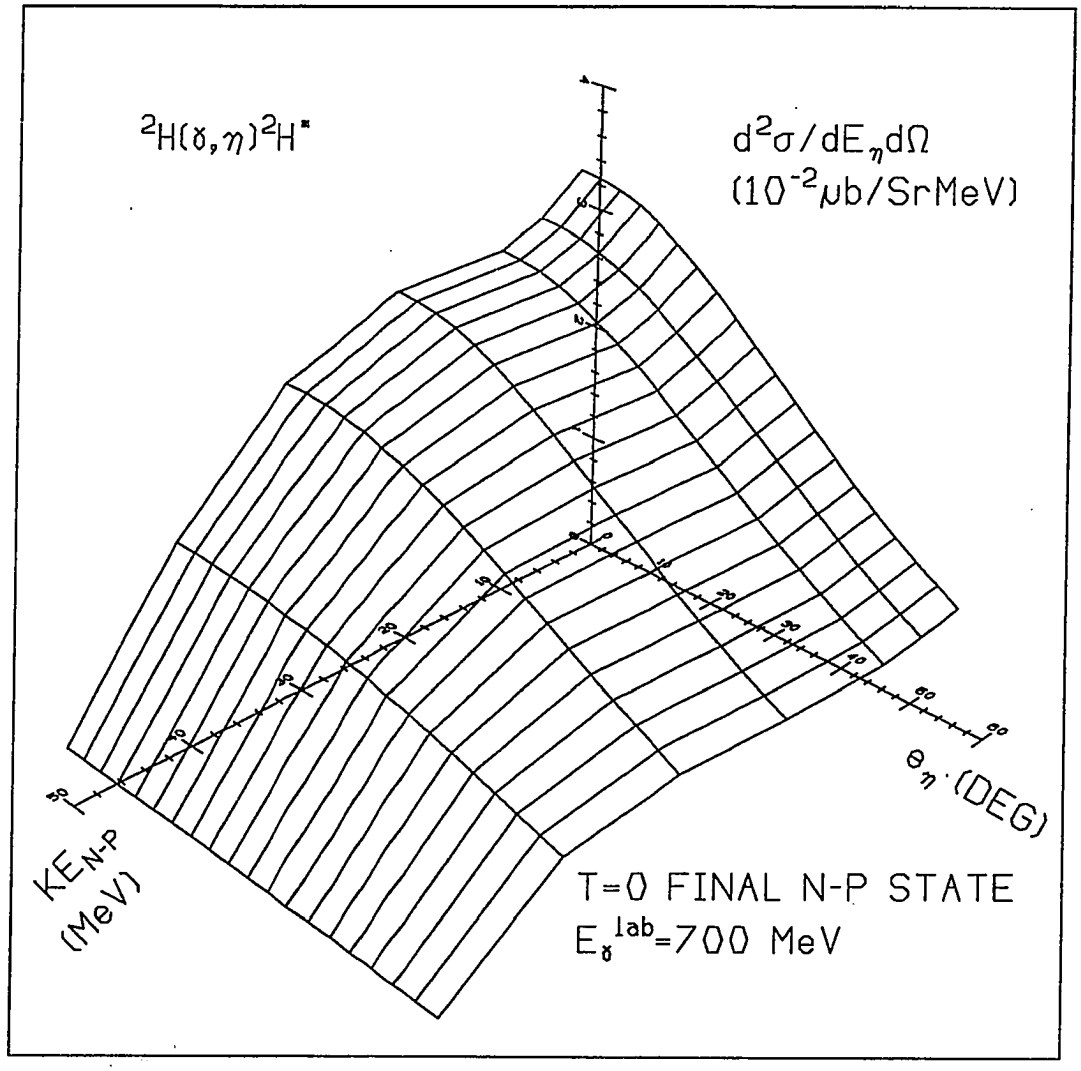

Figure 6. The T=0 Cross Section as a Function of Eta Angle and n-p Relative Kinetic Energy at E_γ^{lab}=700 *MeV*.

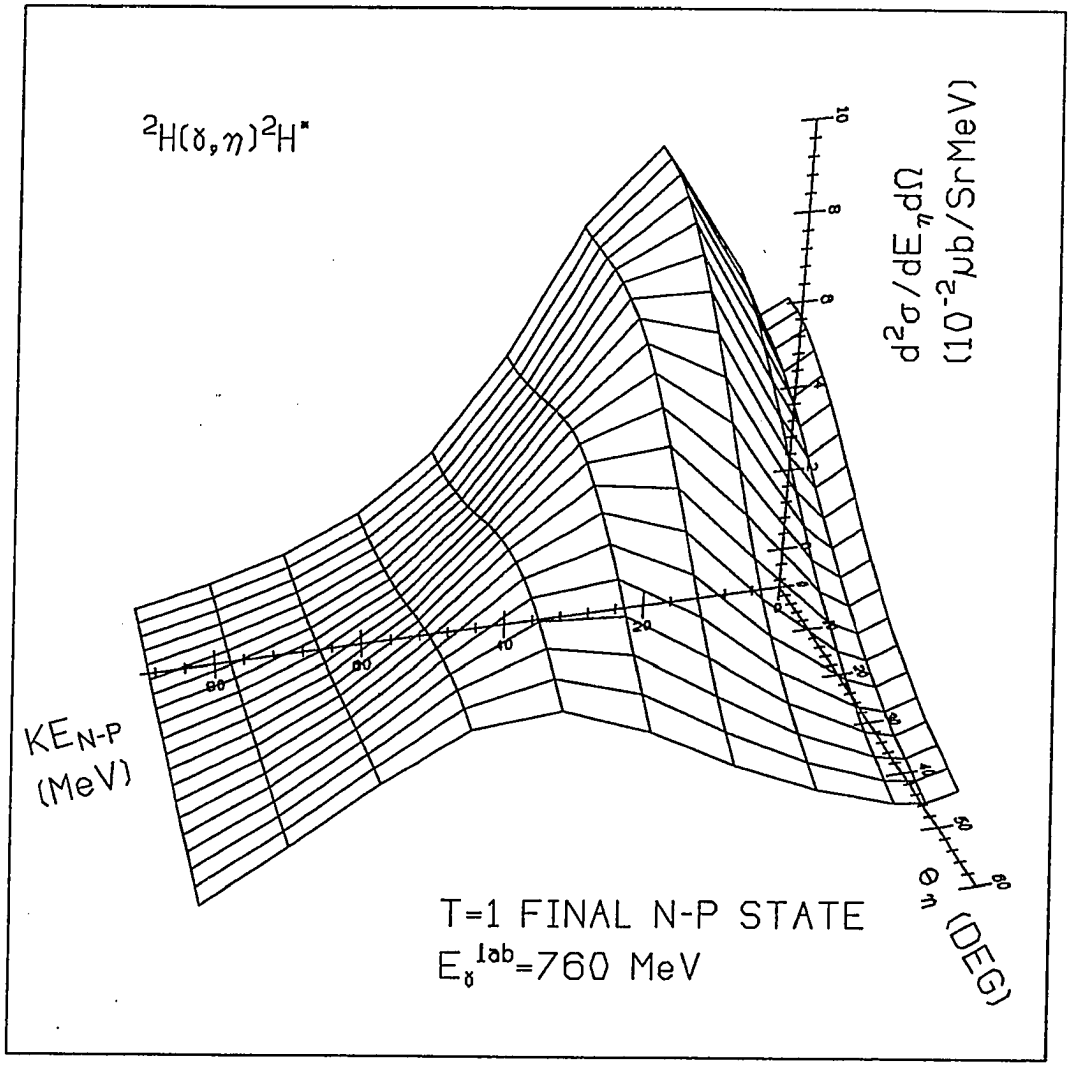

Figure 7. The T=1 Cross Section as a Function of Eta Angle and n-p Relative Kinetic Energy at E_γ^{lab}=760 *MeV*.

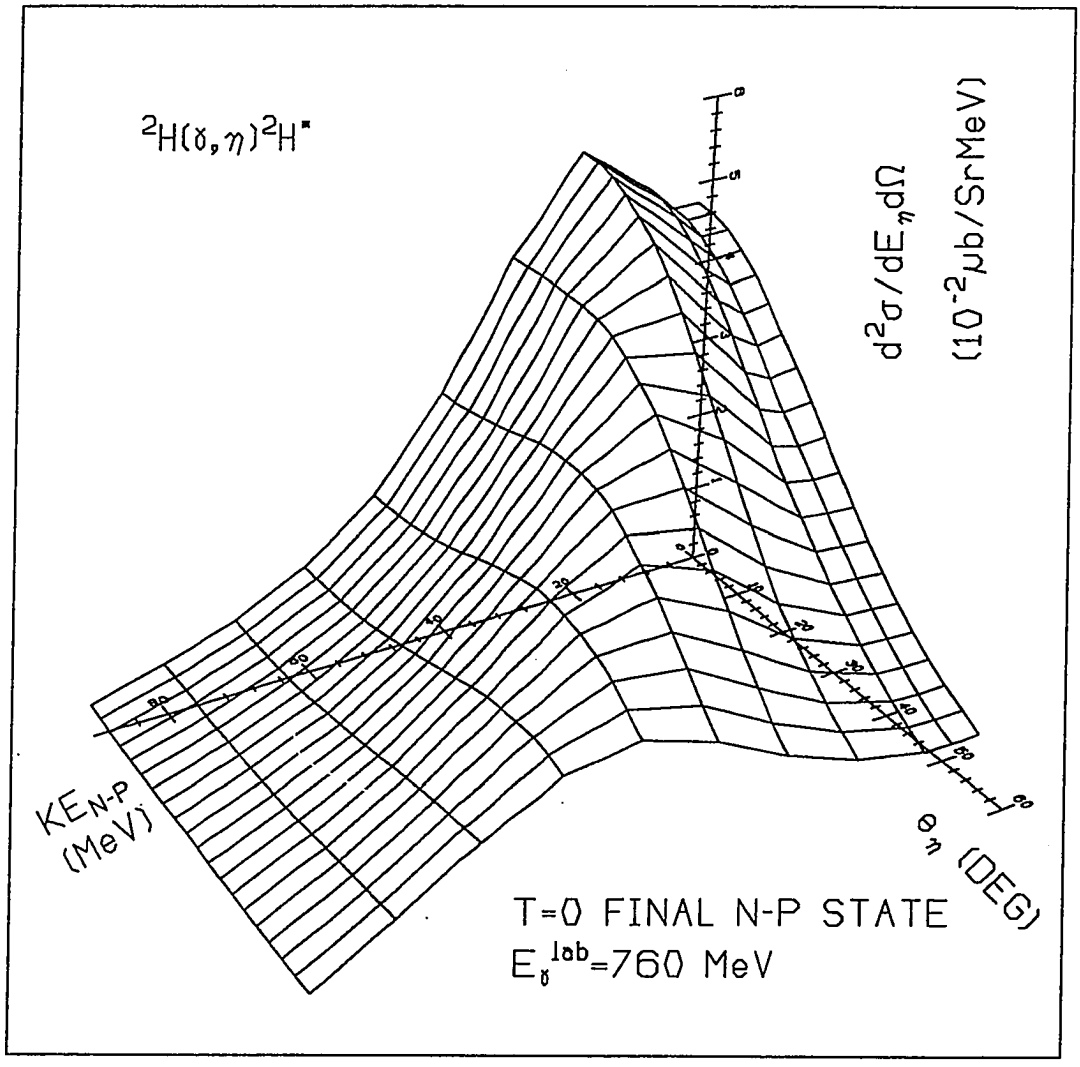

Figure 8. The T=0 Cross Section as a Function of Eta Angle and n-p Relative Kinetic Energy at E_γ^{lab}-760 *MeV*.

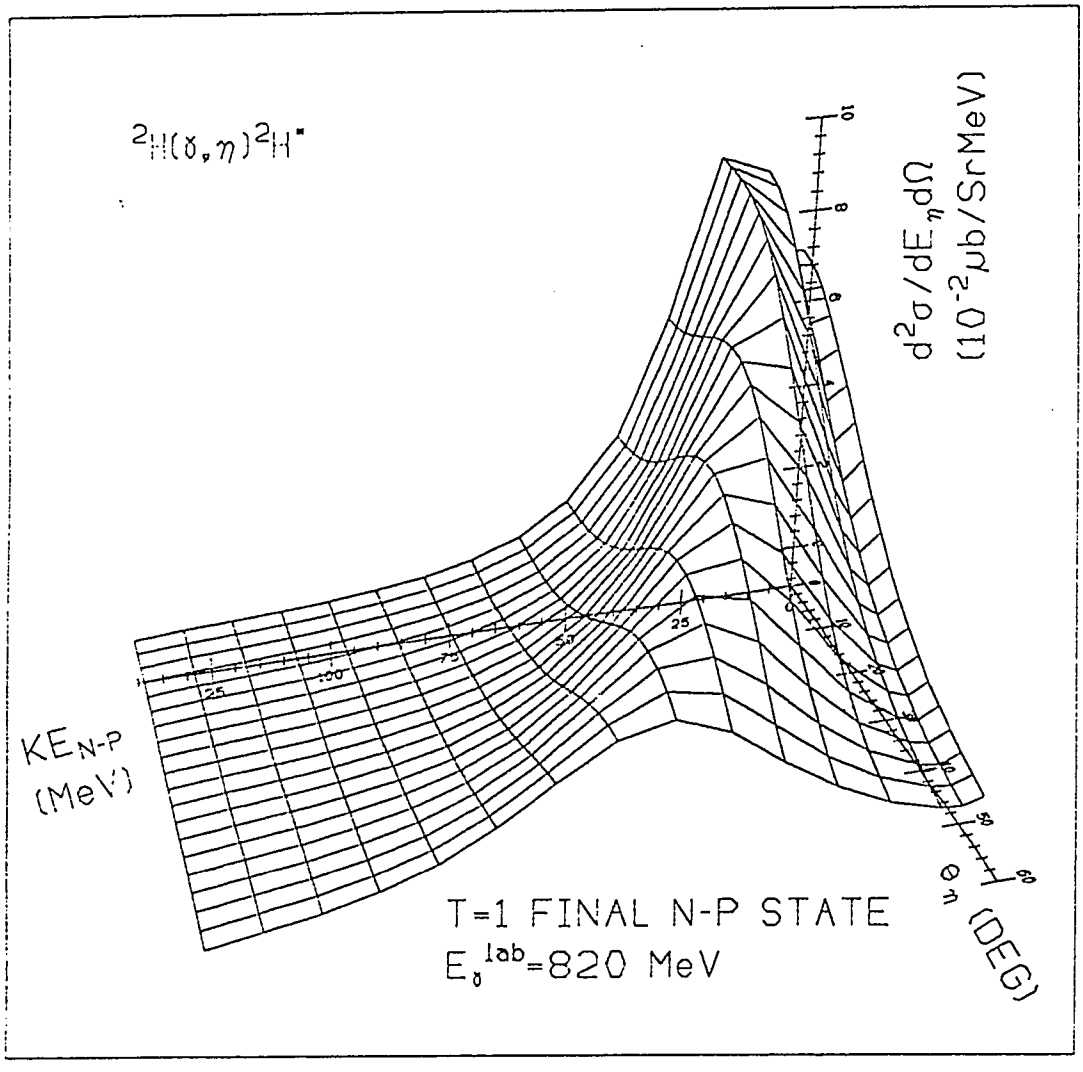

Figure 9. The T=1 Cross Section as a Function of Eta Angle and n-p Relative Kinetic Energy at E_γ^{lab}=820 *MeV*.

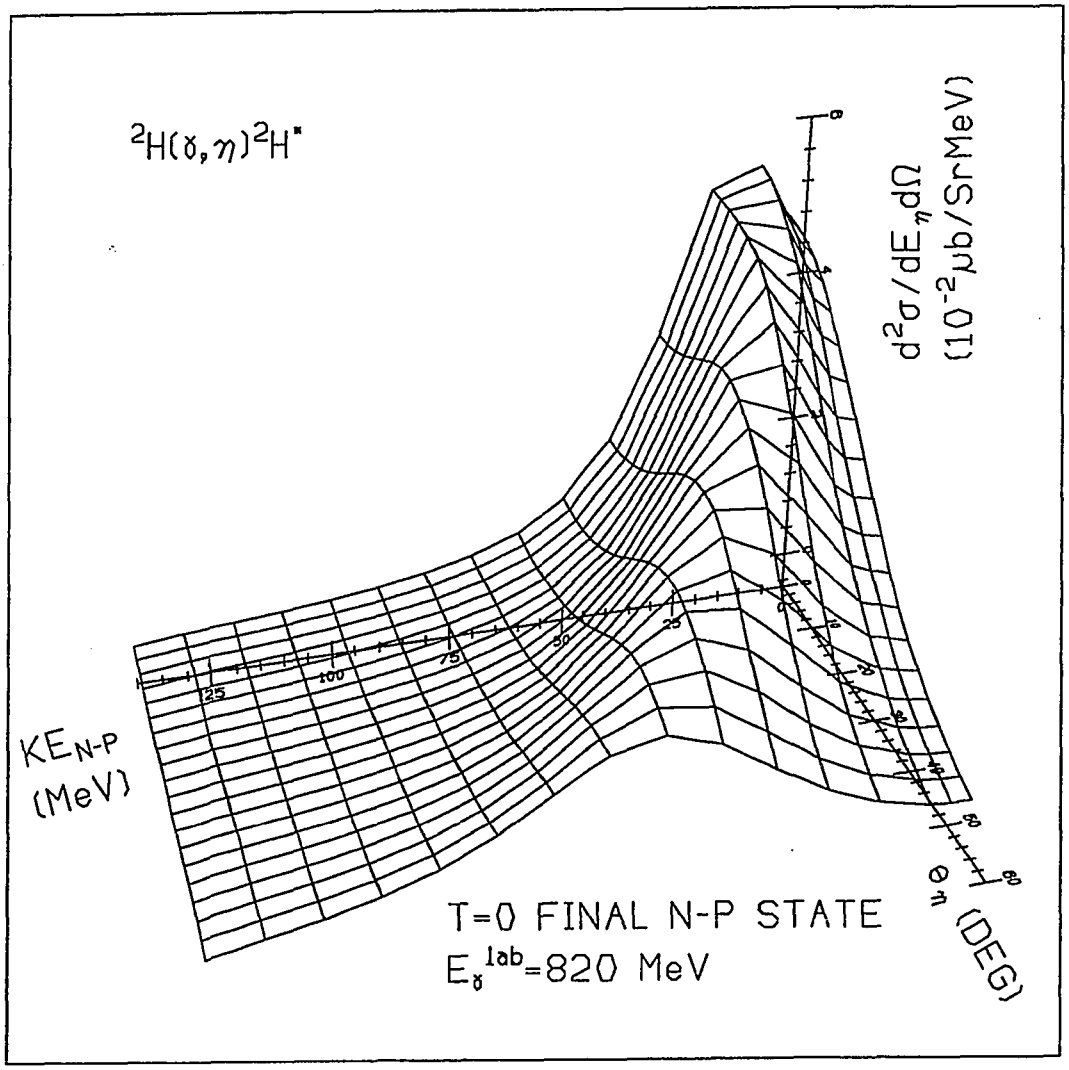

Figure 10. The T=0 Cross Section as a Function of Eta Angle and n-p Relative Kinetic Energy at E_γ^{lab}=820 *MeV*.

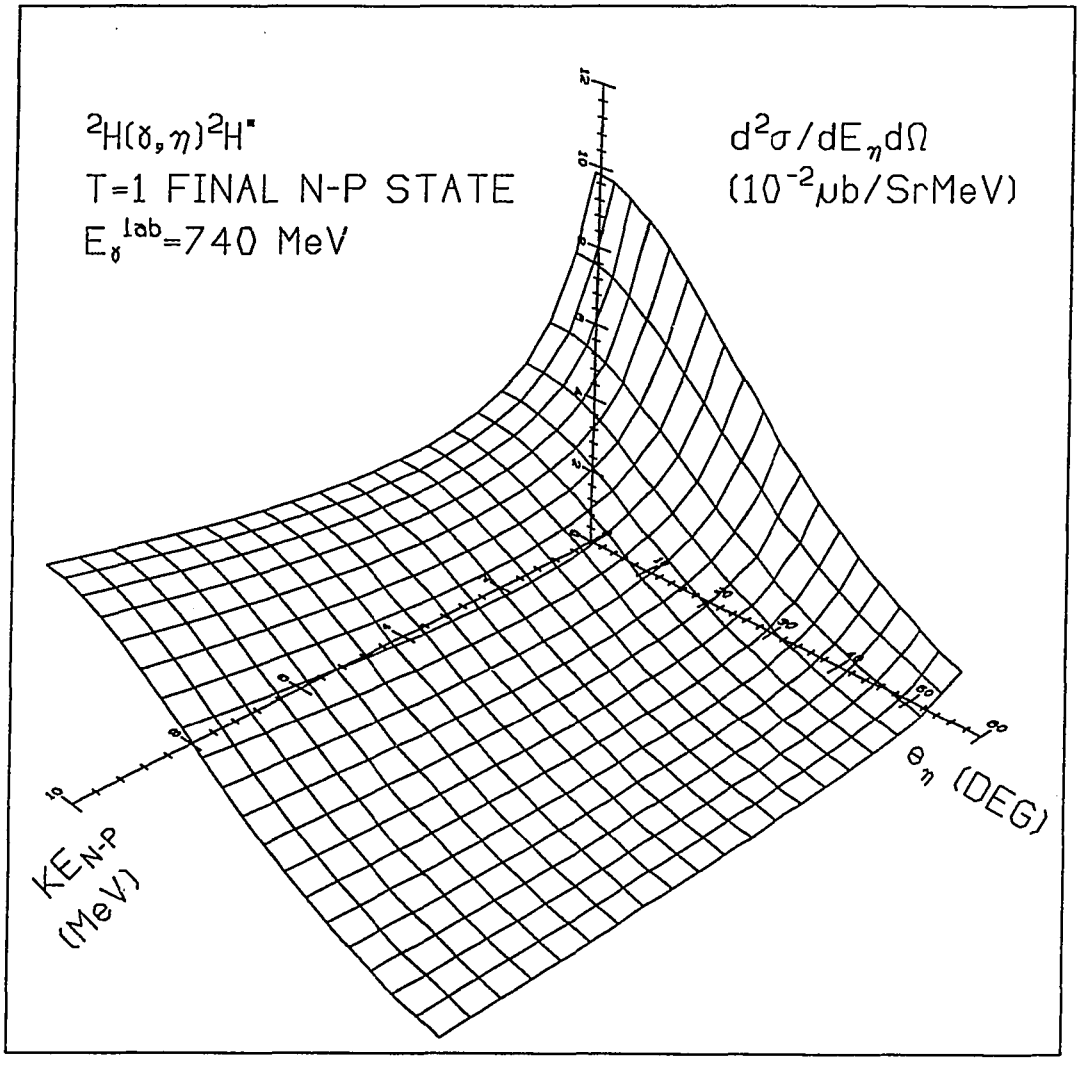

Figure 11. The T=1 Cross Section as a Function of Eta Angle and n-p Relative Kinetic Energy from 0 to 10 MeV at E_γ^{lab}=740 *MeV*.

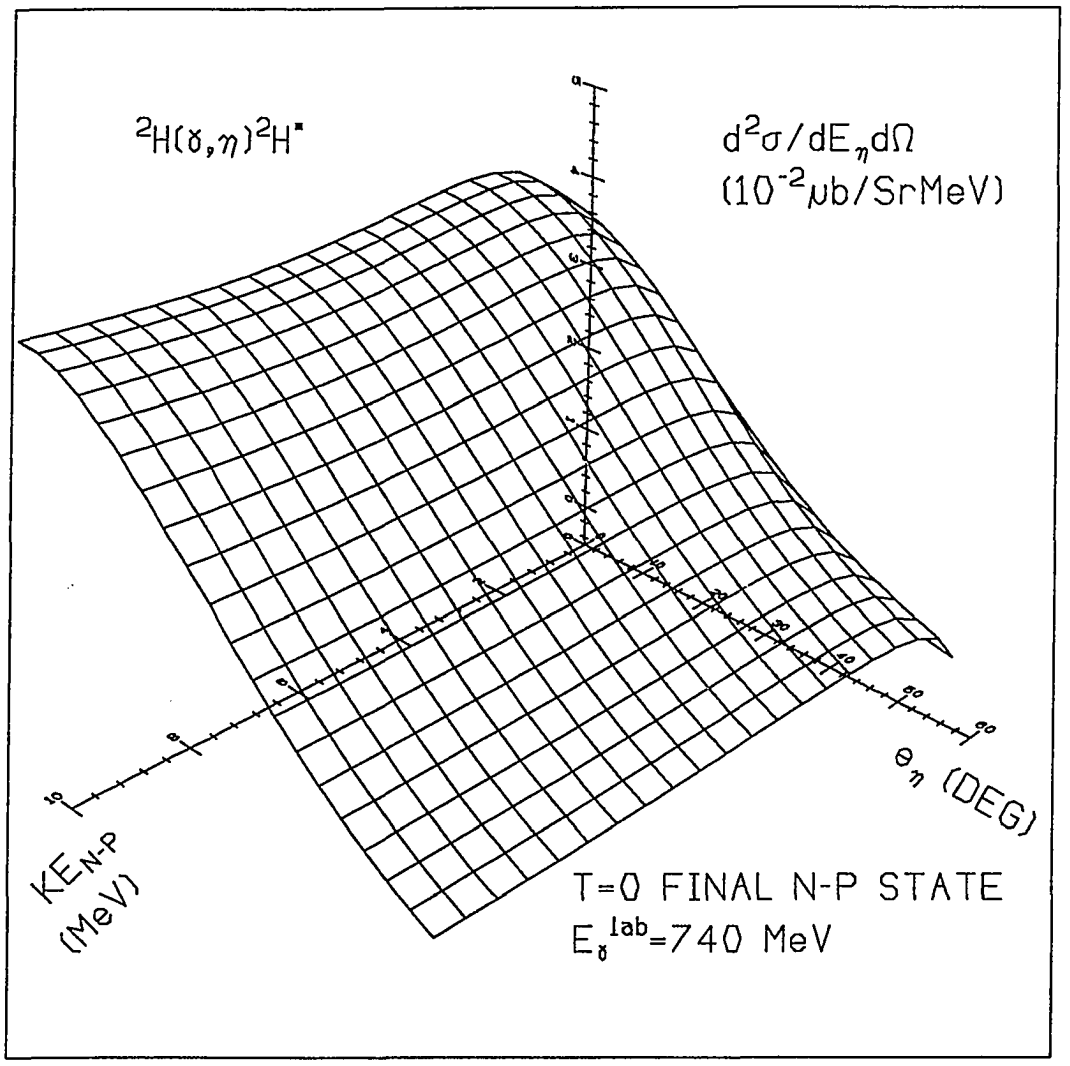

Figure 12. The T=0 Cross Section as a Function of Eta Angle and n-p Relative Kinetic Energy from 0 to 10 MeV at E_γ^{lab}=740 *MeV*.

these two groups of figures, one finds that cross sections of T=0 and T=1 final channels are of very similar shape at n-p relative kinetic energies beyond 10 MeV, yet very different below 10 MeV. Figures 11 and 12 are quite typical. Cross sections at other photon energies from 640 to 900 MeV have shapes very similar to that in Figures 11 and 12. This work then concentrates on the region where n-p relative kinetic energy is smaller than 10 MeV, with the purpose of distinguishing between isovector and isoscalar electromagnetic transition amplitudes. One should note that $F_c^p - F_c^n$ yields only T=0 cross sections, while $F_c^p - -F_c^n$ yields only T=1 cross sections.

The dependences of cross sections on n-p relative kinetic energies are given for both T=0 and T=1 channels in Figures 4 and 13 at θ_η=0 degrees for several photon energies. Cross sections calculated by Lorentz transforming $\hat{k}_c'$ from $\hat{k}'$ are also given by dotted curves in Figure 4 (Please refer to the discussion in the last section in Chapter III). The very different dependence on n-p relative kinetic energy between T=0 and T=1 cross sections indicates that the isospin nature of the S_{11} transition amplitude may be determined by measuring zero-degree eta cross sections at the photon energy where the S_{11} resonance dominates. One thing worth mentioning here is that this

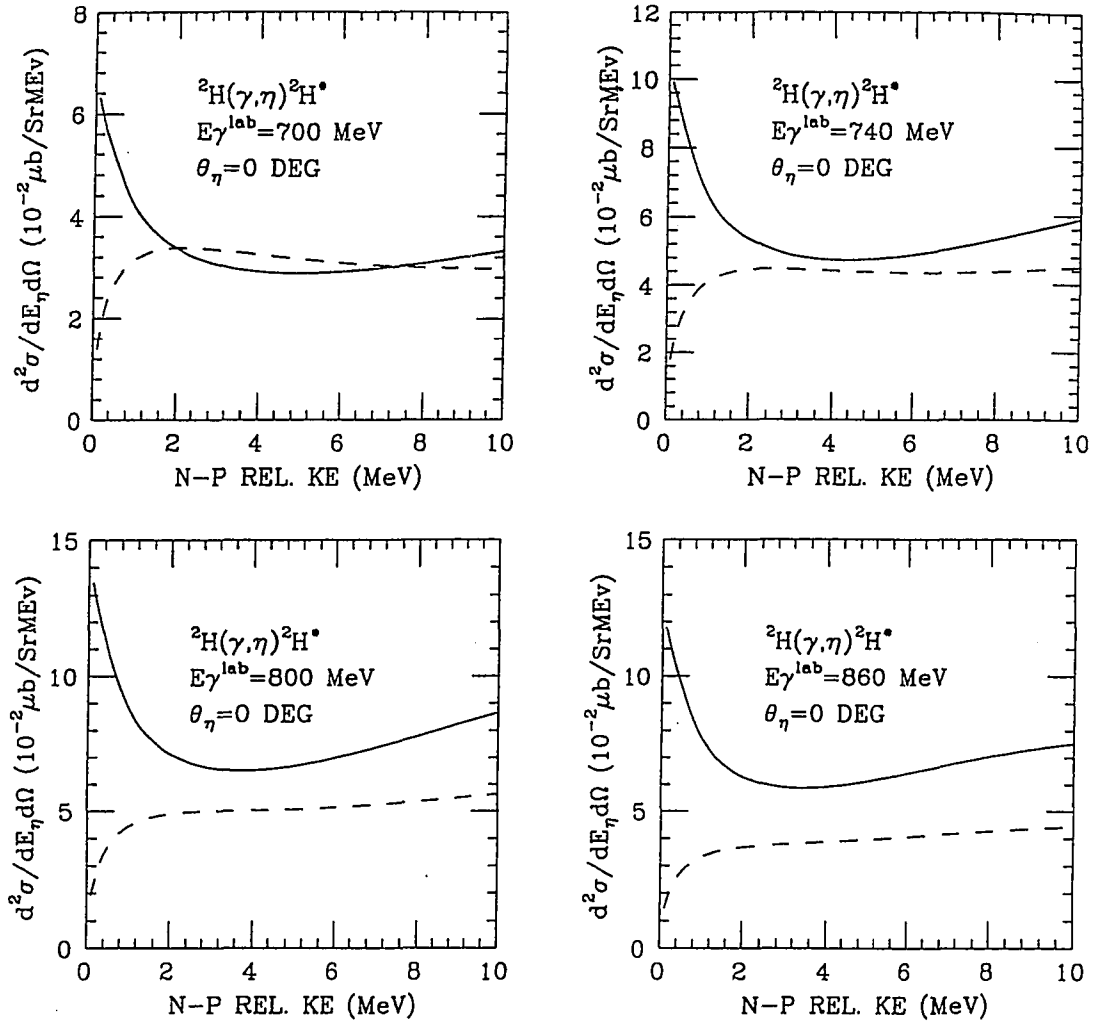

Figure 13. Both T=1 (Solid Curves) and T=0 (Dashed Curves) Cross Sections, at Zero Degrees and Several Incident Photon Energies, as Functions of n-p Relative Kinetic Energy.

calculation is only accurate at forward angles (see also the discussion in the last section of Chapter III).

Figures 3 and 14 shows the angular distribution at several incident photon energies. The n-p relative kinetic energies are chosen to give large cross sections. The angular distribution does not distinguish between the T=0 and T=1 final channels. However, it peaks at forward angles where the forward angle approximation is valid. At 40 degrees the cross section drops by about 50%. Again the dotted curves in Figure 3 give the results with Lorentz transformed $\hat{k}'_c$. The discussion in the last section of Chapter III indicates that the cross section at high photon energy is not sensitive to the angle transformation employed.

The effects of eliminating the S_{11} contribution from the elementary amplitudes are shown in Figures 15 and 16, where cross sections at zero degrees for both T=0 and T=1 final n-p states are plotted versus incident photon energy. Calculations with and without Fermi-averaging the elementary amplitudes are also included in Figures 15 and 16. The Fermi-averaging reduces the cross section by 20-30%, but does not smear out the contribution from the S_{11} as much as in the photonuclear calculations.[8] The S_{11} is demonstrated to dominate the eta cross section in E_γ^{lab}~740 *MeV* region (up to 60-70%), while at around 800 MeV

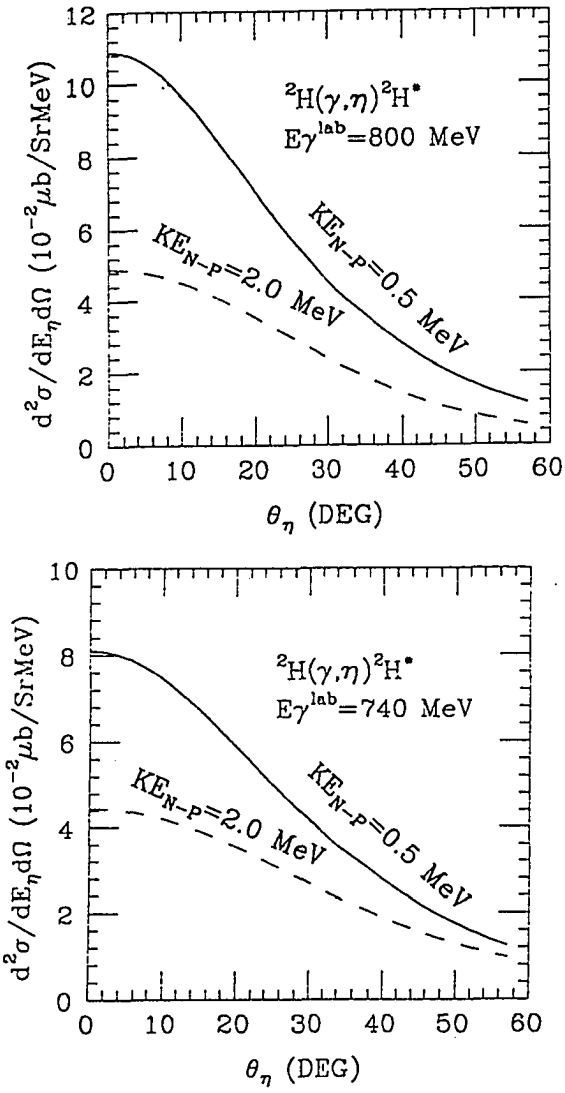

Figure 14. The Angular Distribution at Selected KE_{N-P} Values and Selected Incident Photon Energies for Both T=1 (Solid Curves) and T=0 (Dashed Curves) Final States.

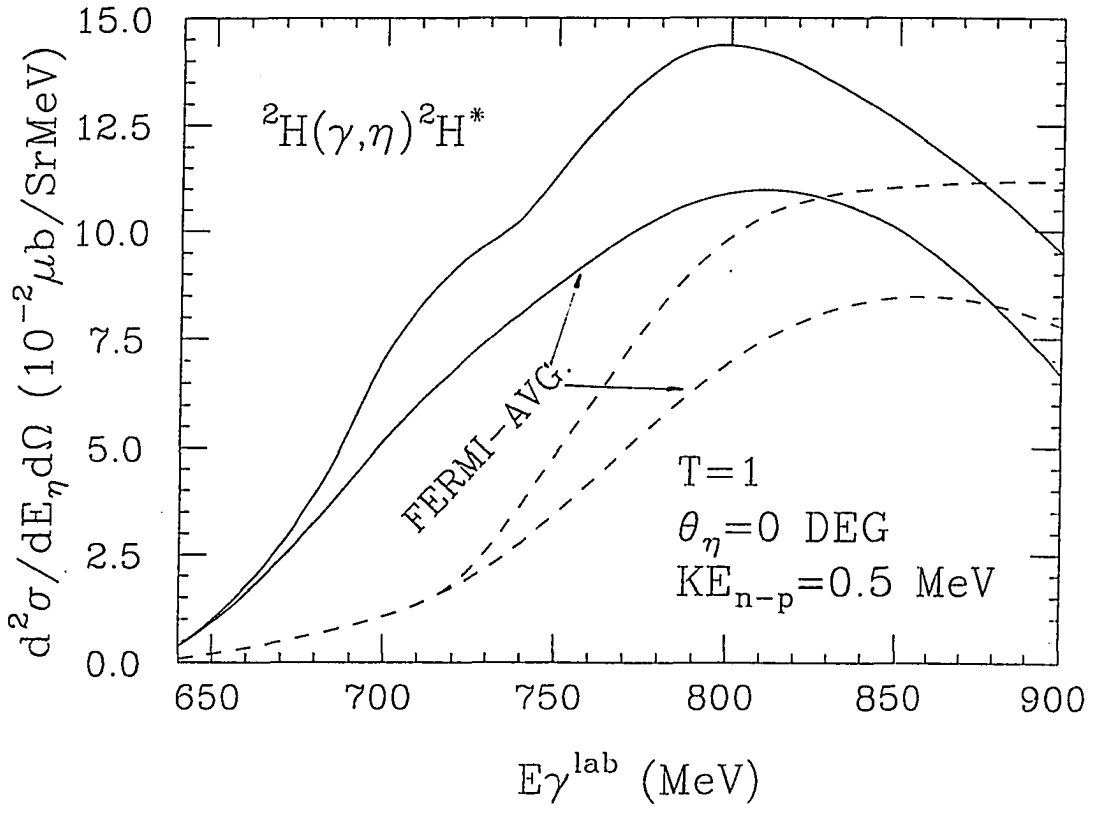

Figure 15. T=1 Cross Section at 0 Degrees and KE_{N-P}=0.5 MeV as a Function of Incident Photon Energy Both With and Without Fermi-averaging the Elementary Amplitudes. Solid Curves are With Full Amplitudes. Dashed Curves are Without the S_{11} Contribution.

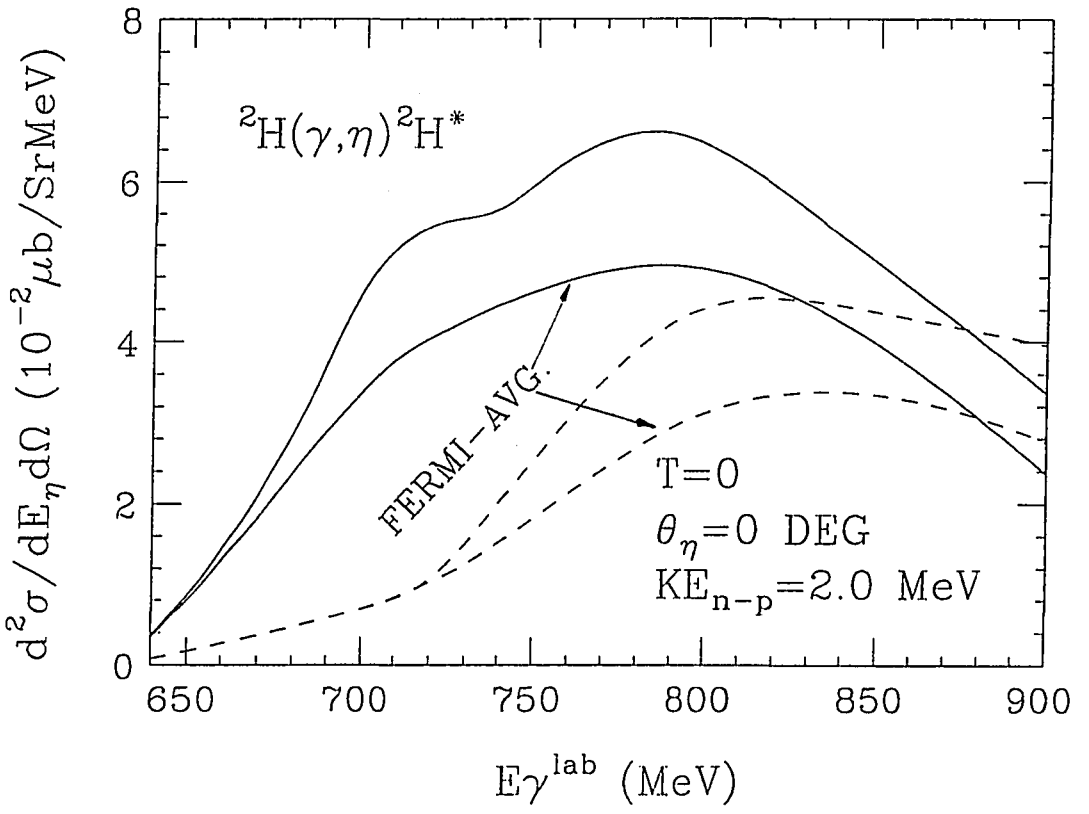

Figure 16. T=0 Cross Section at 0 Degrees and KE_{N-P}=2.0 MeV as a Function of Incident Photon Energy Both With and Without Fermi-averaging the Elementary Amplitudes. Solid Curves are With Full Amplitudes. Dashed Curves are Without the S_{11} Contribution.

photon laboratory energy, where the peak of the cross section occurs, it accounts for only 30-40% of the cross section. The reason is that at E_γ^{lab}-740 *MeV*, the total energy of photon and the nucleon in the γN c.m. (2CM) frame is 1507 MeV, almost on the resonance position of the S_{11} in Cutkosky resonances.[12] In this reaction one may want to concentrate on the photon energy near 740 MeV.

Finally, Figure 17 displays the T=0 and T=1 cross sections at zero degrees and E_γ^{lab}-740 *MeV* which have been folded with a Gaussian width of 1 MeV to simulate the detector resolution. The T=0 curve also includes the impulse approximation prediction for the $^2H(\gamma,\eta)^2H$ cross section calculated by assuming F_c^p-F_c^n. Even with the simulated detector resolution, one can still distinguish between the pure isoscalar and pure isovector amplitudes from the cross section.

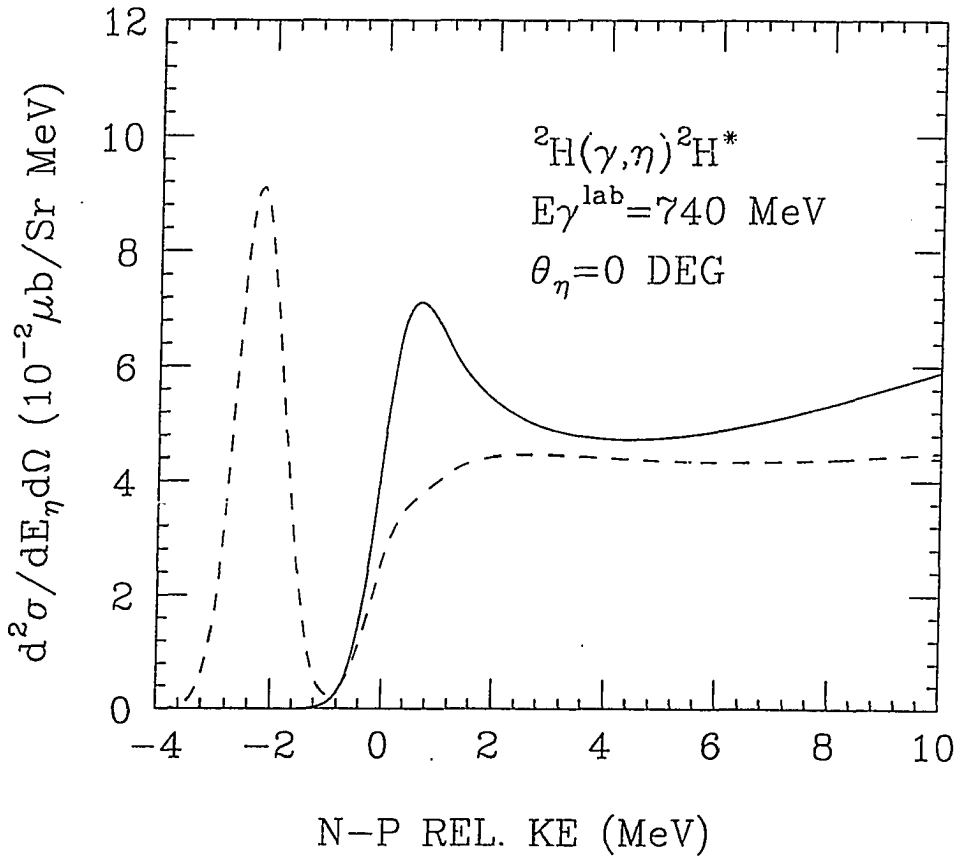

Figure 17. Cross Sections Folded With a Gaussian of 1 MeV Width at 0 Degrees and E_γ^{lab}=740 *MeV* as Functions of n-p Relative Kinetic Energy. The Solid Curve is T=1 Cross Section. The Dashed Curve is T=0 Cross Section Which Also Includes the Impulse Approximation Prediction of the $^2H(\gamma,\eta)^2H$ Cross Section.

CHAPTER V

CONCLUSION

Calculations for the $^2H(\gamma,\eta)^2H^*$ reaction have been performed in the plane-wave impulse approximation with a recent fit[9] to the elementary $\gamma+p\rightarrow\eta+p$ amplitude, and with describing the n-p final state interaction by Reid's soft core potentials.[10] The S_{11} resonance is demonstrated to dominate the cross section in the region of 740 MeV incident photon energy. There is a small difference between calculations with and without Fermi-averaging the elementary amplitude. The loosely bounded deuteron does not smear out the contributions from individual nucleon resonances as much as was determined for heavier nuclei.[8] The deuteron breakup can accommodate higher momentum transfer than in the reaction $^2H(\gamma,\eta)^2H$, and therefore, produces larger total cross sections. One can also expect that the recattering effect is negligible compared to the single scattering because of the deuteron breakup. Cross sections calculated by assuming pure isoscalar and isovector elementary amplitudes exhibit very different dependence on the n-p relative kinetic energy at zero degrees. These results suggest that the $^2H(\gamma,\eta)^2H^*$ reaction may provide a signature for the isospin components of the

S_{11} electromagnetic transition amplitude. This will complement measurements for $^2H(\gamma,\eta)^2H$ which can proceed only through the isoscalar components of the transition operator.

Appendix A

Calculation of Reduced Matrix Elements

The reduced matrix element $\langle (Y_l \otimes \frac{1}{2})^{j'} \| X^J \| (Y_{l_i} \otimes \frac{1}{2})^{j} \rangle$ in the third section in Chapter III is given below.

If $X^J_{m_J} = Y_{lm}(\hat{r})$, then the unreduced matrix element is

$$\langle (Y_l \otimes \frac{1}{2})^{j'}_{m'_j} | Y_{lm} | (Y_{l_i} \otimes \frac{1}{2})^{j}_{m_j} \rangle$$

$$- \sum_{m' m'_p m_i m_p} \langle l' m' \tfrac{1}{2} m'_p | j' m'_j \rangle \langle l_i m_i \tfrac{1}{2} m_p | j m_j \rangle \langle Y_{l'm'} \chi_{m'_p} | Y_{lm} | (Y_{l_i m_i} \chi_{m_p} \rangle$$

$$- \sum_{m' m_i m_p} \langle l' m' \tfrac{1}{2} m_p | j' m'_j \rangle \langle l_i m_i \tfrac{1}{2} m_p | j m_j \rangle \langle Y_{l'm'} | Y_{lm} | Y_{l_i m_i} \rangle \ . \qquad (1)$$

From the identities and definitions (b) and (d) in Chapter III, the above equation becomes

$$\langle (Y_l \otimes \frac{1}{2})^{j'}_{m'_j} | Y_{lm} | (Y_{l_i} \otimes \frac{1}{2})^{j}_{m_j} \rangle$$

$$- \frac{\hat{l}\hat{l}_i}{\sqrt{4\pi}\hat{l}'} \langle l 0 l_i 0 | l' 0 \rangle (-1)^{l' - \frac{3}{2} + 2m'_j + 2m_j + j - l} \hat{j}\hat{l}' \begin{Bmatrix} l' & j' & \frac{1}{2} \\ j & l_i & l \end{Bmatrix} \cdot$$

$$\cdot \langle j m_j l m | j' m'_j \rangle \ . \qquad (2)$$

By the definition (f) in Chapter III, together with eq. (2), the reduced matrix element of $Y_{lm}(\hat{r})$ is finally given as

$$\frac{1}{\hat{J}}\langle (Y_l \otimes \frac{1}{2})^{j'} \| Y_l \| (Y_{l_i} \otimes \frac{1}{2})^{j} \rangle$$

$$= \frac{1}{\sqrt{4\pi}} \hat{l}\hat{l}_i\hat{j}(-1)^{j-l_i-\frac{3}{2}} \langle l0 l_i 0 | l'0 \rangle \begin{Bmatrix} l' j' \frac{1}{2} \\ j\ l_i\ l \end{Bmatrix} . \qquad (3)$$

For $X^J_{m_J} = [Y_l \otimes \sigma]^J_{m_J}$, the situation is more complicated. First, for a general irreducible tensor operator, from the definition (f) in Chapter III and orthogonality of Clebsch-Gordan coefficients, one has

$$\frac{1}{\hat{k}}\langle j' \| T^k \| j \rangle = \frac{[k]}{[j']} \sum_{m_j m'_j} \langle j m_j k q | j' m'_j \rangle \langle j' m'_j | T^k_q | j m_j \rangle . \qquad (4)$$

For a tensor product X^k composed of irreducible tensor operators $T^{k_1}_{q_1}$ and $U^{k_2}_{q_2}$ acking on different parts of a system, identity (g) in Chapter III and the above equation give

$$\frac{1}{\hat{K}}\langle j'_1 j'_2 J' \| X^K \| j_1 j_2 J \rangle$$

$$= \frac{[K]}{[J']} \sum_{\substack{MM' q_1 q_2 \\ m'_1 m'_2 m_1 m_2}} \langle JMKQ | J'M' \rangle \langle j'_1 m'_1 j'_2 m'_2 | J'M' \rangle \langle j_1 m_1 j_2 m_2 | JM \rangle \cdot$$

$$\cdot \langle k_1 q_1 k_2 q_2 | KQ \rangle \langle j'_1 m'_1 j'_2 m'_2 | T^{k_1}_{q_1} U^{k_2}_{q_2} | j_1 m_1 j_2 m_2 \rangle , \qquad (5)$$

while

$$\langle j_1' m_1' j_2' m_2' | T^{k_1}_{q_1} U^{k_2}_{q_2} | j_1 m_1 j_2 m_2 \rangle$$

$$-\frac{1}{\hat{k}_1 \hat{k}_2} \langle j_1 m_1 k_1 q_1 | j_1' m_1' \rangle \langle j_2 m_2 k_2 q_2 | j_2' m_2' \rangle \langle j_1' \| T^{k_1} \| j_1 \rangle \cdot$$

$$\cdot \langle j_2' \| U^{k_2} \| j_2 \rangle \ . \qquad (6)$$

From eqs. (5) and (6) together with the following identity:

$$\begin{Bmatrix} j_{11} & j_{12} & j_{13} \\ j_{21} & j_{22} & j_{23} \\ j_{31} & j_{32} & j_{33} \end{Bmatrix}$$

$$= \sum_{all\, m's} \begin{pmatrix} j_{11} & j_{12} & j_{13} \\ m_{11} & m_{12} & m_{13} \end{pmatrix} \begin{pmatrix} j_{21} & j_{22} & j_{23} \\ m_{21} & m_{22} & m_{23} \end{pmatrix} \begin{pmatrix} j_{31} & j_{32} & j_{33} \\ m_{31} & m_{32} & m_{33} \end{pmatrix} \cdot$$

$$\cdot \begin{pmatrix} j_{11} & j_{21} & j_{31} \\ m_{11} & m_{21} & m_{31} \end{pmatrix} \begin{pmatrix} j_{12} & j_{22} & j_{32} \\ m_{12} & m_{22} & m_{32} \end{pmatrix} \begin{pmatrix} j_{13} & j_{23} & j_{33} \\ m_{13} & m_{23} & m_{33} \end{pmatrix},$$

one finally reaches

$$\frac{1}{\hat{K}} \langle j_1' j_2' J' \| X^K \| j_1 j_2 J \rangle$$

$$= (-1)^{\hat{K}} \frac{\hat{J}_1' \hat{J}_2'}{\hat{K}_1 \hat{K}_2} \begin{Bmatrix} j_1' & j_1 & k_1 \\ j_2' & j_2 & k_2 \\ J' & J & K \end{Bmatrix} \langle j_1' \| T^{k_1} \| j_1 \rangle \langle j_2' \| U^{k_2} \| j_2 \rangle \ . \qquad (7)$$

By using eq. (7) and following result:

$$\langle l' \| Y_l \| l_i \rangle = \frac{[l]\hat{l}_i}{\sqrt{4\pi}\hat{l}'} \langle l 0 l_i 0 | l' 0 \rangle ,$$

and

$$\langle \frac{1}{2} \| \sigma \| \frac{1}{2} \rangle = 3 ,$$

the reduced matrix element of $X^J_{m_J} = [Y_l \otimes \sigma]^J_{m_J}$ is finally obtained as

$$\frac{1}{\hat{J}} \langle (Y_l \otimes \frac{1}{2})^{j'} \| [Y_l \otimes \sigma]^J \| (Y_{l_i} \otimes \frac{1}{2})^j \rangle$$

$$= \sqrt{3}\hat{j}\hat{J}\frac{\hat{l}\hat{l}_i}{\sqrt{2\pi}} \begin{Bmatrix} l' & l_i & l \\ \frac{1}{2} & \frac{1}{2} & 1 \\ j' & j & J \end{Bmatrix} \langle l 0 l_i 0 | l' 0 \rangle . \qquad (8)$$

REFERENCES

1. J. C. Peng, Pion-induced Meson Productions in Nuclei- the (π,η) and the (π^+,K^+) Reactions. Proc. Int. Symp. on Medium Energy Phys., Eds. H. C. Chiang and L. S. Zheng, World Scientific, 336 (1987).

2. W. J. Metcalf and R. L. Walker, A Phenomenological Analysis of Pion Photoproduction. Nucl. Phys. **B76**, 253 (1974).

3. R. Koniuk and N. Isgur, Baryon Decays in a Quark Model With Chromodynamics. Phys. Rev. **D21**, 1868 (1980).

4. F. Foster and G. Hughes, Electroproduction of Nucleon Resonances. Rep. Prog. Phys. **46**, 1445 (1983).

5. R. L. Anderson and R. Prepost, Coherent Photoproduction of the η^0 Meson From Deuterium. Phys. Rev. Lett. **23**, 46 (1969).

6. N. Hoshi, H. Hyuga and K. Kubodera, Coherent Photo $-\eta$ production on the Deuteron. Nucl. Phys. **A324** (1979) 234.

7. D. Halderson and A. S. Rosenthal, Eta Photoproduction on the Deuteron. Nucl. Phys. **A501**, 856 (1989).

8. D. Halderson and A. S. Rosenthal, Photoproduction of Eta-mesons From Nuclei. Phys. Rev. **C42**, 2584 (1990).

9. F. Tabakin, S. A. Dytman and A. S. Rosenthal, Photo- duction of eta Mesons. Excited Baryons 1988, Eds. G. Adams, N. C. Mukhopadhyay, and P. Stoler, World Scientific, 168 (1988).

10. R. V. Reid, Local Phenomenological Nucleon-Nuclson Potentials. Ann. of Phys. **50**, 411 (1968).

11. M. L. Goldberger and K. M. Watson, Collision Theory. New York: John Wiley & Sons, 1964.

12. Review of Particle Properties. Phys. Lett. **B170**, 1 (1986).

13. H. R. Hicks, **et al.**, Isobar Analysis of $\gamma p \rightarrow \eta p$. Phys.

Rev. D7, 2614 (1973).